Aus dem Bereich Medizinische Biochemie und Molekularbiologie
Theoretische Medizin und Biowissenschaften
der Medizinischen Fakultät
der Universität des Saarlandes, Homburg/Saar

Analysis of tissue specific MIC60 isoforms 1 and 3 in human cells and mice

Dissertation zur Erlangung des Grades einer Doktorin der Medizin der Medizinischen Fakultät
der UNIVERSITÄT DES SAARLANDES
2021

vorgelegt von: Sonja Zimmermanns
geb. am: 21.10.1997 in Karlsruhe

Tag der Promotion: 31.05.2021

Dekan: Univ.-Prof. Dr. med. Michael D. Menger

Prüfer: Prof. Dr. Martin van der Laan

Prof. Dr. Peter Lipp

Table of Content

Table of Figures and Tables:

Abbreviations

°C	degree Celsius
µg	microgram
µl	microlitre
µm	micrometre
Amp	ampicillin
Anti-MIC10	antibody against MIC10
Anti-MIC60	antibody against MIC60
Anti-SAM50	antibody against SAM50
ATP	adenosine-5'-triphosphate
ATP5B	human ATP synthase subunit β
BN-PAGE	blue native polyacrylamide gel electrophoresis
cm	centimetre
CO-IP	co-immunoprecipitation
COX	cytochrome-C oxidase
dH_2O	distilled water
DMEM	Dulbecco's Modified Eagle's Medium
DNA	deoxyribonucleic acid
DNAJC11	human DnaJ homolog subfamily C member 11
DRP1	dynamin-related protein 1
ER	endoplasmic reticulum
FBS	fetal bovine serum
FLAG-tag	FLAG peptide at C-terminus
h	hour(s)
HEK293T cells	human embryonic kidney cells 293T
IM	inner mitochondrial membrane
IMS	intermembrane space
kDa	kilo Dalton
l	litre
LB	lysogeny broth
m	mouse
mA	milliampere
mDNAJC11	mouse DnaJ homolog subfamily C member 11
mg	milligram
MIB	mitochondrial intermembrane space bridging complex
MIC60.1	human MIC60 isoform 1

MIC60.1-F	human MIC60 isoform 1 tagged with FLAG-peptide
MIC60.3	human MIC60 isoform 3
MIC60.3-F	human MIC60 isoform 3 tagged with FLAG-peptide
MICOS	mitochondrial contact site and cristae organizing system
MICX	human MICOS protein with the approximately mass of X kDa in yeast
min	minutes
ml	millilitre
mM	millimole
mMIC60.1	mouse MIC60 isoform 1
mMIC60.3	mouse MIC60 isoform 3
mMICX	mouse MICOS protein with the approximately mass of X kDa in yeast
mQIL1	mouse MICOS complex subunit 13 (MIC13)
mRNA	messenger ribonucleic acid
mSAMX	mouse SAM protein with the approximately mass of X kDa in yeast
mSLC25A46	mouse solute carrier family 25 member 46
mtDNA	mitochondrial deoxyribonucleic acid
mTOM	mouse TOM protein with the approximately mass of X kDa in yeast
mV	millivolt
mVDAC	mouse voltage-dependent anion-selective channel protein 1
OM	outer mitochondrial membrane
QIL1	MICOS complex subunit 13 in human (MIC13)
RBM20	RNA-binding motif protein 20
RNA	ribonucleic acid
SAM	sorting and assembly machinery
SAMX	human SAM protein with the approximately mass of X kDa in yeast
SDS-PAGE	sodium dodecyl sulphate polyacrylamide gel electrophoresis
SLC25A46	solute carrier family 25 member 46
TOM	translocase of the outer membrane
TOMX	human TOM protein with the approximately mass of X kDa in yeast
VDAC	voltage-dependent anion-selective channel protein 1
WT	wild type
xg	times gravity
y	yeast
yMICX	yeast MICOS protein with the approximately mass of X kDa in yeast

1. Abstract

Mitochondria are essential organelles of eukaryotic cells. They fulfil multiple functions, including metabolism and signalling between other cell organelles. Mitochondria are surrounded by two lipid bilayers, an outer and an inner membrane, that separate the intermembrane space and the matrix. The inner mitochondrial membrane is highly folded and divided into the inner boundary membrane and invaginations termed cristae. They are connected by tube-like membrane structures termed crista junctions, which are generated and stabilised by the mitochondrial contact site and cristae organizing system (MICOS) complex. The core subunit of the MICOS complex is the subunit MIC60, which stabilises the membrane curvature at crista junctions and forms the connection of inner and outer mitochondrial membrane. In the absence of MIC60, the mitochondrial ultra-structure is disrupted and there is a decrease in crista junction formation and stability. When looking at MICOS complex function, there is a variety of diseases linked to malfunction of MICOS subunits such as Down Syndrome, Parkinson's disease and epilepsy.
Different isoforms of MIC60 have been identified and it has been proposed that different tissue types express different MIC60 isoforms. So far, it is unclear whether those isoforms differ in their biochemical properties. Furthermore, RNA sequencing of patient tissue suffering from familiar dilatative cardiomyopathy revealed mutations of the splicing factor RNA-binding motif protein 20 (RBM20). RBM20 mutation potentially leads to an alternative splicing of the MIC60 gene in cardiomyocytes, resulting in the expression of MIC60 isoform 1 instead of MIC60 isoform 3 in healthy cardiomyocytes.

In this thesis, two lines of experiments, one with different mouse tissues and one with human embryonic kidney cells (HEK293T cell) were carried out. First, different mouse tissues were analysed regarding their expression of MIC60 isoforms in healthy brain, heart and skeletal muscle cells. Additionally, different tissues isolated from wild-type and heterogenic RMB20 mutated mice were used to examine the expression of MIC60 isoforms and MICOS complex proteins in heart and brain cells. The difference in MIC60 isoform expression depending on the tissue type and the consequences on protein and complex stability of MIC60 interacting proteins was assessed. The second line of experiments focused on the analysis of MIC60 isoforms 1 and 3 and potential changes in MICOS protein and complex stability using HEK293T cells either expressing MIC60 isoform 1 or isoform 3. Furthermore, MICOS interacting proteins, MIC60 protein-protein interaction and the influence on protein import function were analysed to reveal differences between MIC60 isoform 1 and isoform 3 on the protein level.

A tissue specific expression of different MIC60 isoforms was confirmed through the first line experiments. While MIC60 isoform 1 is mainly expressed in brain cells, MIC60 isoform 3 is the dominant variant in heart and skeletal muscle cells. Despite this finding, the protein stability of MICOS

complex and MIC60 interacting proteins appears to be similar. Regarding complex stability, there is a decrease of molecular mass of MICOS complex detectable in cells that express MIC60 isoform 3. Surprisingly, the experiments with tissues from WT and RBM20 mutated mice showed no change of isoforms in the heart cells of heterogenic mutated RBM20 mice. Nevertheless, when comparing healthy heart and brain tissues of the WT mice with respect to the expression of MICOS subunits, remarkable differences were detectable. In brain mitochondria, there is almost no expression of MIC19 while the amount of expressed MIC25 is higher than in heart cells. Also, the amount of MICOS interaction partners DNAJC11 and SCL25A46 in brain cells is higher than in heart cells. Thus, it appears that not only MIC60, but other MICOS components and interaction partners show a tissue specific expression as well.

To sum it up, there is a tissue specificity of MIC60 isoform 1 and 3 expression shown in mouse tissues. Also because of RNA sequencing of human tissue, this leads to the assumption, that not only in mice but also in other animal cells, different tissue types express different isoforms of MIC60. Tissue specificity was also shown for other MICOS proteins. Even though, a difference in cells expressing MIC60 isoforms 1 and 3 was expected, the analysis of human MIC60 isoforms 1 and 3 in HEK293T cells revealed no difference in the examined protein functions and MIC60 protein interactions. Only the decreased MICOS complex stability in cells expressing MIC60.3 indicates a difference in MIC60 isoform function. A follow-up analysis of the MIC60 isoforms as well as a repeated analysis of RBM20 tissue concerning MIC60 isoforms should be addressed by more detailed experiments in the future. A further focus of interest should be the tissue specificity of different MICOS components and possible changes in mitochondrial function.

Analyse der gewebsspezifischen MIC60 Protein Isoformen 1 und 3 in menschlichen Zellen und in Mausgewebe

Eukaryotische Zellen, die Grundbausteine des menschlichen Lebens, sind zusammengesetzt aus multiplen Zellorganellen. Mitochondrien sind maßgeblich am Zellmetabolismus, der Synthese von ATP und den Signalwegen zwischen Zellorganellen beteiligt. Damit sind sie essenzieller Bestand jeder eukaryotischen Zelle. Die bohnenförmigen Organellen werden von einer Lipiddoppelschicht umrandet. Die äußere und die gefaltete innere mitochondriale Membran grenzen den Intermembranraum und den Matrixraum voneinander ab. Diese Faltung der inneren Membran nennt man Cristae. Das Bindeglied zwischen den Cristae und dem restlichen Teil der inneren mitochondrialen Membran sind tunnelartige Membranabschnitte - *Crista Junctions*. Diese *Crista Junctions* werden durch den „mitochondrial contact side and cristae organising system“ (MICOS) Komplex gebildet und ihre Form wird durch den MICOS Komplex aufrechterhalten. Mutationen der einzelnen MICOS Proteine oder Veränderungen des Komplexes führen unter anderem zu Down Syndrom, Parkinson oder auch Epilepsie.
Der MICOS Komplex in menschlichen Zellen besteht aus 7 bekannten Proteinen, von denen MIC60 die zentrale Untereinheit des MICOS Komplexes darstellt. MIC60 stabilisiert den MICOS Komplex und ist beteiligt an der Aufrechterhaltung der Cristae. Des Weiteren spielt MIC60 eine entscheidende Rolle bei der Verbindung von innerer und äußerer mitochondrialer Membran.
Verschiedene Isoformen von MIC60 konnten genetisch verifiziert werden, und es besteht die Annahme, dass in den Mitochondrien verschiedener Organgewebe unterschiedliche Isoformen exprimiert werden. Ob die Funktion verschiedener Isoformen von MIC60 variiert, ist bisher noch nicht untersucht worden. Die RNA Sequenzierung von Patientenproben mit einer Mutation des RBM20 Splicingproteins zeigte ein alternatives Splicen des MIC60 Gens, was zu einer Expression von MIC60 Isoform 1 anstelle von MIC60 Isoform 3 im menschlichen Herzen führen soll. Mutationen von RBM20 sind verknüpft mit Familiärer Dilatativer Kardiomyopathie.

Der Fokus dieser Arbeit liegt auf zwei Experimentreihen, mit dem Ziel, die Expression von verschiedenen MIC60 Isoformen in verschiedenen Organgeweben zu beweisen und mögliche Unterschiede in den Funktionen von MIC60 Isoformen 1 und 3 zu analysieren. Dafür wurde Organgewebe von gesunden Mäusen speziell auf ihre MIC60 Isoformen analysiert und dann MIC60 und MICOS Komplex Proteine des Gewebes von gesunden und RBM20 heterogen mutierten Mäusen verglichen. Die zweite Experimentreihe untersucht HEK293T Zellen, bei denen zuerst die Expression von MIC60 unterdrückt, und danach eine spezifische Expression von MIC60 Isoformen 1 und 3 mit und ohne FLAG-peptid induziert wurde. Diese Zelllinien wurden verwendet, um die Proteinfunktion der MICOS Untereinheiten spezifischer untersuchen zu können.

Die durchgeführten Experimente zeigten, dass die Isoformen von MIC60 gewebsspezifisch exprimiert werden. In den Mitochondrien der Mausgehirnzellen findet sich MIC60 Isoform 1. Im Vergleich dazu exprimieren die Mitochondrien in Mausherzen und im Skelettmuskel MIC60 Isoform 3.
Die Analyse der verschieden MIC60 Isoformen in HEK293T Zellen zeigte im Vergleich dazu keinen signifikanten Unterschied der MIC60 Isoformen auf Proteinebene. Auffallend war jedoch die Verminderung der Proteinmasse des MICOS Komplexes in Zellen mit MIC60 Isoform 3.
In den Mitochondrien der Herzzellen der WT und RBM20 heterogen mutierten Mäusen konnten, anders als erwartet, kein Unterschied in der exprimierten MIC60 Isoform gefunden werden. Der Vergleich von MICOS Komplex Proteinen in den Herz- und Gehirnmitochondrien zeigte eine gewebsspezifische Expression für die Proteinmengen von MIC19, MIC25 und DNAJC11. In den Gehirnzellen zeigte sich eine sehr geringe Expression von MIC19 und im Vergleich dazu eine wesentlich höhere Expression von MIC25. Des Weiteren zeigten sich größere Mengen an exprimierten DNAJC11 und SLC25A46, bekannten Interaktionspartnern des MICOS Komplexes, in Gehirnzellen. Dies führt zu der Annahme, dass nicht nur MIC60 Isoformen, sondern auch andere MICOS Komponenten und Interaktionspartner gewebsspezifisch exprimiert werden.

Schlussendlich lässt sich, auch aufgrund von RNA Sequenzierung des MIC60 Proteins in menschlichem Gewebe, vermuten, dass eine gewebespezifische Expression von MIC60 Isoformen nicht nur in verschiedenen Mausgeweben, sondern auch in anderen tierischen und in menschlichem Gewebe stattfindet. Es scheint wahrscheinlich, dass auch die anderen MICOS Komponenten gewebsspezifisch in unterschiedlichen Mengen exprimiert werden.
Trotz dieser Gewebsspezifität von MIC60 Isoformen 1 und 3 konnten auf der untersuchten Proteinebene keine Unterschiede in der MICOS Proteinstabilität und Proteininteraktion festgestellt werden. Funktionsunterschiede der MIC60 Isoformen 1 und 3 scheinen dennoch wahrscheinlich, da Zellen, die MIC60 Isoform 3 exprimieren, eine Veränderung der MICOS Komplexstabilität aufweisen. Eine tiefergehende Analyse der Gewebsspezifität der einzelnen MICOS Untereinheiten, speziell auch der MIC60 Isoformen und deren potentielle Funktionsunterschiede, als auch eine erneute Versuchsreihe mit RBM20 mutierten Zellen sollte in Zukunft angestrebt werden.

2. Introduction

2.1. Eukaryotic cells and their organelles

The cell is the smallest unit of life. Prokaryotic cells like bacteria are single cell organisms with a diameter of about 1-5 micrometre (µm), they are not compartmentalised and their deoxyribonucleic acid (DNA) floats inside the cytoplasm, forming a nuclear region. In comparison, eukaryotic cells have a complex, compartmentalised structure and are surrounded by the plasma membrane consisting of phospholipids, cholesterol, glycolipids and various proteins. Most eukaryotic cells, including all animal and human cells, have a diameter of about 10-100µm and contain different cell organelles performing different functions. The cell organelles, small compartments inside the cell, can be found inside the cytosol. Some organelles appear only once in each cell while others can be found multiple times. The largest cell organelle is the nucleus containing the cell's genome. There is one Golgi apparatus mainly for transport of proteins inside the cell via exocytosis and one endoplasmic reticulum (ER) as a central part of the protein synthesis pathway for membrane and secretory proteins and the synthesis of membrane lipids.

Mitochondria are eukaryotic cell organelles known as the "powerhouse" of the cell. Depending on the respective cell type, there is a variable number of single mitochondria or huge mitochondrial networks inside the eukaryotic cells. About 99% of the mitochondrial proteome is nuclear encoded and transported into the mitochondria. But mitochondria also have their own mitochondrial DNA (mtDNA) which in humans encodes for 13 proteins that are expressed within the matrix of the organelle. The mitochondrial functions include metabolism, synthesis of ATP by oxidative phosphorylation and signalling processes inside the cell. These functions can be efficiently performed because of the spatial organisation of mitochondrial protein complexes and mitochondrial membranes, which leads to maximal efficiency.[13,40,43,44,46–48,52]

Mitochondria are cell organelles surrounded by two lipid bilayers, the outer mitochondrial membrane (OM) and the inner mitochondrial membrane (IM). For this reason, the endosymbiotic theory states, that mitochondria evolved from prokaryotic cells which have been engulfed by prokaryotic cells.[39,64,78] Inside the mitochondria a second lipid bilayer, the IM, separates the intermembrane space (IMS), between OM and IM, and the matrix inside the mitochondria. The IM can be further divided in the inner boundary membrane and invaginations termed cristae which are essential for surface enlargement. Cristae are membrane stacks connected to the inner boundary membrane by tube-like membrane structures called crista junctions. The characteristic architecture of the highly folded IM is maintained with the help of "mitochondrial contact site and cristae organizing system" (MICOS) and F_1F_o-ATP synthase.

While the MICOS complex generates and stabilises the crista junctions, the formation of cristae rims and tubes is promoted by oligomerized F_1F_o-ATP synthase. Mainly F_1F_o-ATP synthase produces ATP, which is used in all cell organelles for energy consuming processes, by oxidative phosphorylation of ADP.[29,34,38,40,70]

2.2. Organisation and function of the MICOS complex

The MICOS complex is a large protein complex composed of inner membrane proteins facing towards the intermembrane space and proteins in the IMS (see Figure 1). [31,38,51] It is crucial for the formation of crista junctions; therefore it is essential for the characteristic IM architecture. In yeast six subunits (yMICX) have been described - yMIC60, yMIC10, yMIC12, yMIC19, yMIC26 and yMIC27. A depletion of one of these subunits in yeast leads to a reduction of cristae junctions and therefore to an aberrant lamellar structure of the mitochondria. [9,38,70,72,74–76]

The human MICOS complex has a mass of about 700 kilo Dalton (kDa) which was determined by blue native polyacrylamide gel electrophoresis (BN-PAGE). It is composed of at least seven proteins (MICX), including MIC60, MIC10, MIC19, MIC26 and MIC27 homologous proteins of the ones in yeast and two additional proteins, QIL1/MIC13 and MIC25 (see Figure 1). QIL1 in humans is distantly related to yMIC12 and MIC25 is a paralog to the MIC19 protein. [7,20,25,30,31,70]

In humans, not all MICOS subunits seem to be essential for the cristae junction formation. With certainty, the depletion of the human subunits MIC60, MIC10, MIC19 and QIL1 leads to a reduced number of cristae junctions and a loss of the characteristic IM architecture. Also, each protein forming the MICOS complex performs individual functions like interaction with different protein complexes of the inner and outer mitochondrial membrane.[7,9,20,30,31,48,75]

Figure 1
Schematic sketch of the human mitochondrial contact side and organising system (MICOS).
Human MICOS consists of at least 7 proteins – MIC10, MIC19, MIC25, MIC26, MIC27, MIC60 and QIL1
OM – outer mitochondrial membrane
IMS – intermembrane space
SAM – sorting and a machinery
IM – inner mitochondrial membrane
M – mitochondrial matrix
DNAJC11 – DnaJ homolog subfamily C member 11

Independent studies identified MIC60, MIC19 and MIC25 as the MIC60 subcomplex of MICOS with a mass of about 450-600 kDa (see Figure 1, red). A second MIC10 subcomplex is formed by MIC10 as core protein together with MIC26, MIC27 and QIL1 (see Figure 1, orange). The MIC10 subcomplex binds to and is stabilised by the MIC60 subcomplex.[20,25,31,72,74,76]

Each subcomplex has different functions, related to the associated proteins, but both subunits together are necessary for formation and maintenance of the crista junctions. In addition, the MIC60 subcomplex interacts with SAM and TOM, two protein complexes of the outer membrane.[24,37,54,60,72,74]

MIC60, the core protein of the MIC60 subunit, is a membrane protein anchored in the inner mitochondrial membrane that spans the intermembrane space. It was first described 1994 by Icho et al. in human heart cells and was named differently in the past 25 years including Mitofilin or Fcj1 before an uniform nomenclature was introduced by Pfanner et al. in 2014. [26,51] MIC60 is a central protein of the MICOS complex, as its depletion in yeast cells leads to a destabilisation of the MICOS complex and to a loss of the characteristic mitochondrial cristae structure. Therefore, it was concluded that the main function of MIC60 is cristae formation and stabilisation. Furthermore, MIC60 interacts with SAM50 an outer membrane protein connecting inner and outer membrane, implicating a direct connection of the different mitochondrial compartments.[15,25,34,37,38,49,54,70]

MIC19 is a protein in the intermembrane space which is able to bind to the inner mitochondrial membrane. MIC19 has a molecular mass of about 26kDa in humans. In human mitochondria MIC19 directly interacts with MIC60 as well as SAM50 in human mitochondria. The knockdown of MIC19 in human cells showed a fragmentation and clustering of mitochondria around the nucleus. Furthermore, a major remodelling of cristae and crista junctions was observed.[14,48] In addition, there was an overall decrease of MICOS and MIB protein levels, except MIC25, indicating, that MIC19 is also a core protein of the central subunit together with MIC60.[14,31,48,72]

MIC25, a subunit of MICOS in vertebrates, is known to be a paralog of MIC19. MIC25 is a result of MIC19 gene duplication.[45,70] Human MIC25 has a molecular mass of about 26.5 kDa and a similar structure to MIC19. It has been reported to interact with MIC19 and also SAM50.[15] The exact function of MIC25 still has to be defined, but it was shown, that the depletion of MIC25 has no effect on protein levels of MICOS and MIB complex proteins and minor effects on cristae morphology.[6,15,25,31,48,72]

In MICOS the MIC10 subcomplex is composed of the proteins MIC10, QIL1, MIC26 and MIC27, forming around the MIC60 subcomplex. MIC10, the core subunit of the MIC10 subcomplex, is a transmembrane protein located in the inner mitochondrial membrane. It has two transmembrane regions with both termini facing towards the intermembrane space. There are two known isoforms of MIC10, the canonical form has a mass of 8.8kDa.[9,25,31] In yeast, yMIC10 is essential for the formation of the crista junctions and also interacts with F_1F_o-ATP synthase.[9,31] Likewise in human mitochondria, MIC10

is a relevant protein for mitochondrial cristae formation. The knockdown of this protein shows a collapse of crista junctions, but does not affect the protein levels of the MIC60 subcomplex components.[31,37]

QIL 1/MIC13 (in human and mouse) and MIC12 (in yeast) are distantly related to each other and are believed to perform similar functions. QIL1 is known to stabilise the MICOS complex and takes part in the formation of the cristae structure.[7,20,25,70] QIL1 has a mass of about 13 kDa. It is a transmembrane protein located in the inner mitochondrial membrane and faces towards the intermembrane space. The knockdown of QIL1 leads to lower protein levels of MIC10, MIC26 and MIC27 while the protein levels of the MIC60 subcomplex are increased. Therefore, QIL1 is proposed to be essential for the connection of the two MICOS subcomplexes. The depletion of QIL1 also causes a disruption of the characteristic mitochondrial ultra-structure.[20,25,70,75]

The non-glycosylated form of MIC26, as part of the MIC10 subunit, is an apolipoprotein located in the inner mitochondrial membrane.[30] Whether the depletion of MIC26 majorly effects the cristae formation is not clear as different reports described conflicting results. However, the depletion of MIC26 leads to a decrease in levels of MIC10.[30,31,48,70]

MIC27 has a molecular mass of 29.2 kDa. It is an apolipoprotein like MIC26 and a paralog to MIC26.[25,45,67] MIC26 and MIC27 seem to work in an antagonistic way, as MIC27 increases the oligomerization of MIC10, because it is shown to lead to a decrease of MIC10 oligomerisation when being depleted. The depletion of MIC26 is shown to result in increased oligomerisation of MIC10.[53] MIC27 directly interacts with MIC60, MIC10 and SAM50. The depletion of MIC27 does not result in decreased protein levels of MICOS or MIB complex proteins and only slightly affects the cristae formation.[31,48,66,70,75]

2.3. Found and predicted isoforms of MICOS proteins

The core subunit of the MICOS complex is MIC60, which stabilises the membrane curvature at crista junctions and is important for the connection of inner and outer mitochondrial membrane.[31,34,38,74] MIC60 is proposed to appear in different isoforms depending on different tissue types.[17,65,77] While most former articles only refer to two known MIC60 isoforms in humans [31], there are several new studies that have reported the existence of more MIC60 isoforms. [17,65,77] In humans, MIC60 has four known isoforms with 80-83,6 kDa mass and five potential isoforms (see Figure 2).[a] In mouse, there are five known mMIC60 isoforms from 78,7-87,7 kDa mass (see Figure 2).[b]

[a] https://www.uniprot.org/uniprot/Q16891, 16.11.2020
[b] https://www.uniprot.org/uniprot/Q8CAQ8, 16.11.2020

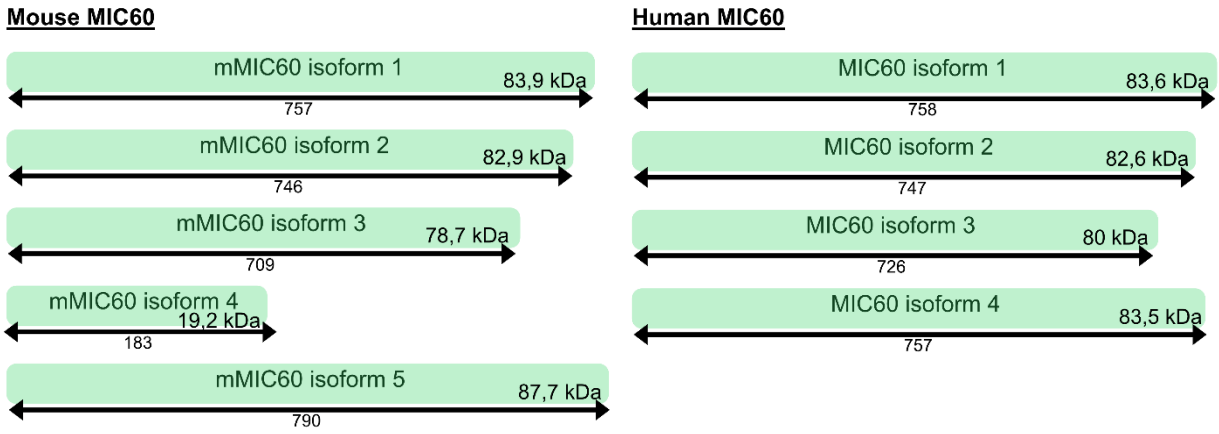

Figure 2
MIC60 isoforms in mouse and human.
Protein mass and amino acid chain length given
Source: https://www.uniprot.org/uniprot/Q16891, 16.11.20 and https://www.uniprot.org/uniprot/Q8CAQ8, 16.11.2020

Not only MIC60 is proposed to appear in different isoforms, but there are described and predicted isoforms of each protein forming the MICOS complex.

Table 1: Described and predicted isoforms of MICOS complex proteins:

human MICOS component	gene name	described protein isoforms	predicted protein isoforms	references
MIC60	IMMT	4	5	https://www.uniprot.org/uniprot/Q16891, 16.11.2020,
MIC19	CHCHD3	1	3	https://www.uniprot.org/uniprot/Q9NX63, 16.11.2020
MIC25	CHCHD6	1	3	https://www.uniprot.org/uniprot/Q9BRQ6, 16.11.2020
MIC10	MICOS10	2	2	https://www.uniprot.org/uniprot/Q5TGZ0, 16.11.2020
QIL1	MICOS13	1	3	https://www.uniprot.org/uniprot/Q5XKP0, 16.11.2020
MIC26	APOO	2	5	https://www.uniprot.org/uniprot/Q9BUR5, 16.11.2020
MIC27	APOOL	1	2	https://www.uniprot.org/uniprot/Q6UXV4, 16.11.2020

Generally speaking, different variants of a protein can be expressed, because of alternative splicing or variable promoter usage. Thus, there is a change in amino acid number possibly leading to modifications of protein conformations. It is known, that protein isoforms can vary in their function and therefore a tissue specificity of protein isoforms can be found.[18,58,62]

One example is the MICOS complex protein MIC26. MIC26 is not only a mitochondrial protein but also a secretory protein. The non-glycosylated isoform of MIC26 is exclusively present in mitochondria while the glycosylated isoform of MIC26 is a apolipoprotein present in light membranes of ER and Golgi apparatus or secreted into the extracellular space as a primary part of high density lipoprotein particles. The expression of the different MIC26 isoforms varies depending on the tissue type. [30,35,73]

Like the MIC26 isoforms, there could be a difference in MIC60 isoforms as well. So far, the different isoforms of MIC60, even though it is an essential protein for the MICOS complex formation, have not been studied in detail. It is unknown whether they differ in their functionality and therefore may influence MICOS proteins, MICOS complex formation and furthermore change the characteristic structure of the mitochondria.

2.4. MICOS interacting proteins

In addition to the interaction of the MICOS subunits with each other, the MICOS complex interacts with several other proteins such as sorting and assembly machinery (SAM), Metaxin 3 and DnaJ homolog subfamily C member 11 (DNAJC11). Together with MICOS they form the 2200 kDa large mitochondrial intermembrane space bridging complex (MIB complex). The MIB complex connects outer and inner membrane, intermembrane space and matrix.[25,49]

The SAM complex in mammalian mitochondria is composed of SAM50, Metaxin 1 and Metaxin 2. It was shown, that SAM50, the core protein of the SAM complex, directly interacts with MIC60 and MIC19. This results in a direct connection of inner and outer mitochondrial membrane. Furthermore, it was shown, that the SAM complex seems to be closely linked to the MICOS complex as it only appears in connection to MICOS and does not appear on its own.[1,32,59,60,68] The main function of the SAM complex is the integration and sorting of β-barrel proteins into the outer mitochondrial membrane. The pore forming subunit of the SAM complex is SAM50. Its depletion leads to a complete loss of cristae and an abnormal mitochondrial morphology. Therefore, the SAM complex seems to be essential for a proper mitochondrial function.[49,60]

DNAJC11 is part of the MIB complex. The knockdown of DNAJC11 leads to no detectable decrease of protein levels in other subunits of the MIB and MICOS complex. However, the DNAJC11 protein level is decreased by the depletion of SAM50. More research on DNAJC11 needs to be done to clarify the exact mitochondrial location and function of this protein in mitochondrial morphology and cristae formation.[27,31,70]

There are several other proteins interacting with the MICOS complex such as the translocase of the outer mitochondrial membrane (TOM) complex, which performs the transport of nuclear encoded preproteins into the mitochondria.[2,11,24,52,69,74] TOM mainly functions as a channel for preproteins encoded by the nuclear DNA. In BN-PAGE, the human TOM complex has a mass of about 380 kDa.[28] Its central proteins TOM20 and TOM22 recognize the preproteins with the help of amino-terminal targeting signals, and TOM40 acts as the channel, importing the preproteins into the intermembrane space. Inside the intermembrane space, the preproteins are further processed and for example integrated into the outer membrane with the help of SAM complex or imported into the mitochondrial matrix.[2,33,41,52,59,69] The MICOS complex, especially the MIC60 subunit, as a TOM and SAM complex binding partner, is

involved in the biogenesis of β-barrel outer membrane proteins.[22,23,38,57,72,76] One example for the function of TOM and SAM complexes is the β-barrel protein voltage-dependent anion-selective channel protein 1 (VDAC). It is located in the outer mitochondrial membrane with a molecular mass of 30.8 kDa. The TOM and SAM complexes together with Metaxins are required for VDAC import and assembly. In human cells, VDAC appears in 3 different isoforms, each isoform functioning differently as they vary in their abilities like Ca^{2+} sensitivity or their pole forming function. Therefore, VDAC is an excellent example for different functioning isoforms in human cells. [22,32,42,52]

The MICOS complex not only interacts with OM proteins and complexes but also with IM complexes such as the dimeric F_1F_o-ATP synthase. The MICOS subunits MIC10 and MIC27 interact with the F_1F_o-ATP synthase. Nevertheless, the stability of the F_1F_o-ATP synthase is not influenced by changes in MICOS proteins.[16,52,53]

Several studies revealed changes in protein levels of MICOS interaction partners when depleting MIC60.[32,38,70] Different MIC60 isoforms potentially not only affect the function of MICOS complex and interaction proteins but could also affect the stability of MIC60 protein-protein interaction. For example, the change of MIC60 isoforms may alter the interaction of the MIB complex proteins, leading to a dysfunction of MIC60, MIC19 and SAM complex interaction.

2.5. Mutations of MICOS subunits and their disease relevance

As mitochondria perform major functions of the cell, mutations of mitochondrial proteins can lead to serious malfunctions with severe patho-physiological consequences. In regard to the MICOS complex various diseases have been associated with mutations in subunits or interacting proteins.

The MIC60-MIC19 subcomplex is connected to disrupted-in-schizophrenia 1 (DISC1), a gene variant that causes schizophrenia. [6,34,50] The first disease related to a disassembly of MICOS complex was found in patients suffering from early-onset fatal mitochondrial encephalopathy with liver disease. Their fibroblasts showed a deletion of QIL1. Due to the loss of QIL1 there was a decrease of MICOS complex subunits and an abnormality in cristae structure.[19,20] The solute carrier family 25 member 46 (SLC25A46) as part of the outer mitochondrial membrane and interaction partner of MIC60 is linked to numerous neurodegenerative diseases. Mutations have been associated with optic atrophy, peripheral neuropathy and ataxia. Furthermore a mutation of SLC25A46 is linked to Charcot-Marie-Tooth neuropathy type 2.[3,4,34] A splicing mutation of DNAJC11, another outer mitochondrial membrane protein, leads to a severe neuromuscular disease in mice. [27,63]

An in-depth analysis of messenger ribonucleic acid (mRNA) isolated from patients with familiar dilatative cardiomyopathy (DCM), revealed a mutation within the RNA-binding motif protein 20 (RBM20).[10] In healthy individuals, RNA sequencing of your research partner [c] has shown, that RMB20 mediates splicing of the sixth exon of the IMMT gene, coding for the MIC60 protein (see Table 1), which leads to the expression of MIC60 isoform 3 (see Figure 3). The mutated RBM20 is severely impaired and therefore the splicing of the sixth exon does not take place, leading to an expression of MIC60 isoform 1.

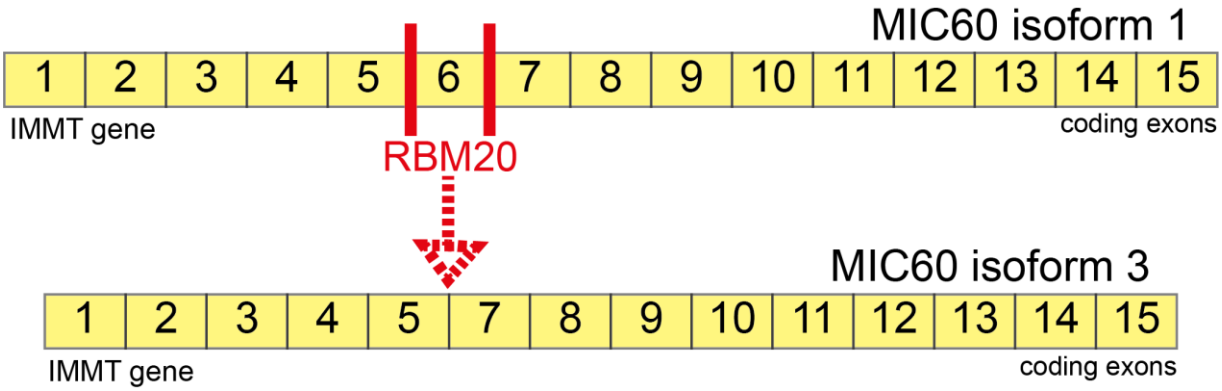

Figure 3
Activity of the RBM20 splicing factor in the IMMT gene coding for MIC60.
The IMMT gene is spliced by the RBM20 splicing factor at exon 6 resulting in the expression of MIC60 isoform 3.

There is a suggestion that healthy human cardiomyocytes mainly express MIC60 isoform 3. A mutation of RMB20 would lead to the expression of MIC60 isoform 1 in cardiomyocytes and is therefore a potential pathogenic factor in familiar DCM.

Alternative splicing of RNA is one way of generating different proteins and leads to genomic diversity. Tissue specific splicing is regulated by splicing factors or regulators like RBM20. In 2012, Guo et al. reported, that there are at least 31 RBM20-dependent genes some of them "involved in bio-mechanics (TTN and TPM1), ion homeostasis and electrical activity (CAMK2D and CACNA1C) and signal transduction (CAMK2D and SPEN)."[21] Studies show a contribution of RBM20 gene editing to cardiac function, as mutations of RBM20 can be linked to cardiac diseases. It was shown, that both, rats and humans with RBM20 missense mutations, suffer from cardiomyopathy and arrhythmia.[10,12,21,36,61]

The familiar DCM caused by RBM20 mutations, mainly in the arginine/serine-rich domain of the RBM20, is associated with young patients and early death. Furthermore, Guo et al. discovered that "RBM20 mutation plays a major role in cardiac adaptive responses mediated by titin (Ttn) and

[c] Information kindly provided by our research partner L.M. Steinmetz from the EMBL Heidelberg/Stanford Genome Technology Center

calcium/calmodulin- dependent protein kinase II (Camk2δ)". [8,10,21,71] In Camk2δ, a mutation of RBM20 results in an exon skipping of Exon 14 and an exon inclusion of exon 15 and 16 resulting in a shift of isoforms from Camk2δB to Camk2δA. For titin, RBM20 mutations lead to the expression of extremely large titin isoforms (N2BA). [21]

As described before, RNA sequencing of our research partner [d] has shown, that RBM20 also modifies the IMMT gene known to code for MIC60. Here, RBM20 leads to an exon skipping of Exon 6.
Therefore, RBM20 mutations also impact the expression of MIC60 isoforms. Whether or not those isoforms contribute to familiar DCM is not examined yet. As mentioned before, little is known about the expression of MIC60 isoforms in different tissue types and about possible changes of protein functions related to different MIC60 isoforms.
The analysis of the characteristics of MIC60 isoforms 1 and 3 is the topic of this thesis. Serving this purpose, MIC60 isoforms in different mouse tissue types are analysed to confirm the expression of MIC60 isoform 3 in healthy cardiomyocytes. Furthermore, HEK293T knockdown MIC60 cells and knockdown MIC60 cells that express MIC60 isoform 1 or MIC60 isoform 3 are analysed in respect of their differences regarding MICOS stability and function. Last but not least, mitochondria were isolated form heart and brain of WT mice and heterogenic mutated RBM20 mice, to analyse the predicted effects of a RBM20 mutation on MIC60 isoforms and possible changes in protein function.

[d] Information kindly provided by our research partner L.M. Steinmetz from the EMBL Heidelberg/Stanford Genome Technology Center

3. Material and Methods

3.1. Cell lines

All cultivated cells used, derived from human embryonic kidney cells 293T (HEK293T) (kindly provided by A. von der Malsburg). Those cells included CRISPR/Cas9 knockdown cells as well as retroviral transduced MIC60 k/d cells that expressed the indicated versions of MIC60.

The HEK293T WT cells were kindly provided by M. Ryan, Deputy Dean of Monash Biomedicine Discovery Institute, Department of Biochemistry & Molecular Biology. The genomic editing was done using the pSpCas9(BB)-2A-GFP CRISPR/Cas9 plasmid (MIC60 guide RNA: CAGCATCTCGGTCAAGCGGA). Then the cells were transfected with the plasmid and FACS-sorted after 48 h. GFP-positive clones were transferred into a 96-well plate. The Clones were screened by western blot and the genomic editing was confirmed by genomic sequencing.[55]

The expression of MIC60 variants was achieved by retroviral transduction (Mo MuLV) of the MIC60 KD cell line followed by selection with puromycin. The locus of the integration was variable and was not determined. The copy number was 1.

Materials:

	origin
3xFLAG peptide	F4799, Sigma Aldrich

Plasmids for retroviral transduction

	origin
pCMV-VSV-G	Addgene, cat. no. 8454
pUMVC (Gag/Pol)	Addgene, cat. no. 8449
pBABE-puro-MIC60.1-FLAG	A. von der Malsburg
pBABE-puro-MIC60.3-FLAG	A. von der Malsburg
pBABE-puro-MIC60.1	A. von der Malsburg
pBABE-puro-MIC60.3	A. von der Malsburg

List of cell lines

	Abbreviations
HEK293T-WT	WT
HEK293T-ΔMIC60	ΔMIC60
HEK293T-ΔMIC60+MIC60.1-FLAG	MIC60.1-F
HEK293T-ΔMIC60+MIC60.3-FLAG	MIC60.3-F
HEK293T-ΔMIC60+MIC60.1	MIC60.1
HEK293T-ΔMIC60+MIC60.3	MIC60.3

HEK293T cells were cultured in Dulbecco's Modified Eagle's Medium (DMEM), supplemented with 10% fetal bovine serum (FBS) and 50 µg/ml Uridine at 37 degree Celsius (°C) with 5% CO_2. The cells were cultivated in 10 centimetre (cm) plates and for experimental use grown in 15cm plates to confluency.

	origin
DMEM	GIBCO ref: 41966-029 Thermo Fischer company
FBS	GIBCO ref: 10270-106 Thermo Fischer company
Uridine	Sigma U3003-5G dissolved in dH_2O and sterile filtered

3.2. Mitochondrial isolation

3.2.1. Mitochondrial isolation from cultured cells

The mitochondrial isolation of cultured cells is based on the procedure used by Acín-Pérez et al.(2008)[5] which is a modified version of Schägger at al. (1995)[56].

The cells were cultured for approximately 3 days at 37°C with 5%CO_2 until confluency (3x15cm plates). Afterwards, cells were collected by rinsing the plates with medium and were then transferred to a falcon tube followed by a centrifugation step at 300 times gravity (xg) for 5 minutes (min). Cells were washed with 10 millilitre (ml) PBS (Phosphate-Buffered Saline, GIBCO 20012-019) and centrifuged again at 300xg for 5min. All remaining liquid was removed, and cell pellets were stored at -80°C.
All steps of the mitochondrial isolation were carried out on ice. Cell pellets were resuspended in 2 ml of low sucrose buffer and transferred into a 5ml glass homogenizer. Cell lysis was achieved with 20 strokes using a drill-fitted pestle. Afterwards an equal volume (2 ml) of medium sucrose buffer was added. The mixture was transferred to microfuge tubes (2 times 2ml) and spun in a centrifuge at 1,000xg

for 5 min at 4°C. After the centrifugation step the supernatant was transferred to clean microfuge tubes and spun again at 12,000xg for 10 min at 4°C. Mitochondrial pellets were resuspended in 300 microlitre (µl) of high sucrose buffer. The protein content was determined by using Bradford protein assay (described in 3.3). Appropriately sized aliquots of purified mitochondria were stored at -80°C.

Buffers:

Low sucrose buffer	83mM Sucrose 10mM HEPES (pH 7.2)
Medium sucrose buffer	250 mM Sucrose 30mM HEPES (pH 7.2)
High sucrose buffer	320 mM Sucrose 1mM EDTA (pH 8.0) 10mM MOPS (pH 7.2)

3.2.2. Mitochondrial isolation from cultured cells specific for Import

The mitochondrial isolation from cultured cells specifically designed for protein import was used to get more purified mitochondria to efficiently perform the protein import afterwards.

Cells were cultured for approximately 2 days till confluency (2 x 14.5cm plates). Then the cells were resuspended in 5 ml PBS (Phosphate-Buffered Saline, GIBCO 20012-019) and pelleted at 800xg for 5 min.

All following steps were carried out on ice or at 4°C. The pellet was resuspended in 2 ml Solution A and transferred into a glass homogenizer. The cells were homogenised with 20 strokes. Afterwards the cells were centrifuged at 800xg for 5 min at 4°C in 2ml tubes. The supernatant was centrifuged at 20,000xg for 10 min at 4 °C. The pellet containing the crude mitochondria was resuspended in 400µl Solution B. For purified mitochondria, the sample was again centrifuged at 20,000xg for 10 min at 4 °C. The final mitochondrial pellet was resuspended in 150µl of Solution B. The protein concentration of the sample was determined by Bradford protein assay (described in 3.3).

Buffers:

Solution A Add fresh before use	20 mM HEPES-KOH (pH 7.6) 220 mM Mannitol 70 mM sucrose 1 mM EDTA (pH 8.0) 2 mg/ml BSA (10xBSA) 0.5mM PMSF
Solution B Add fresh before use	20 mM HEPES-KOH (pH 7.6) 220 mM Mannitol 70 mM sucrose 1 mM EDTA 0.5 mM PMSF
10xBSA	20mg/ml BSA Bovine serum albumin, ChemCruz (Lot:B0416)

3.2.3. Mitochondrial isolation from frozen mouse tissue

The heart and brain tissues were stored at -80°C and the tissue was thawed on ice. The heart ventricles were removed and 1ml BSA/IS was added. Both tissues were homogenised with scissors in the BSA/IS solution and then transferred to lose fitting Teflon/glass dounce homogeniser and homogenised for 7 min. The homogenate was transferred to tight fitting Teflon/glass dounce homogeniser and homogenised with 40 strokes. The homogenate was centrifuged at 1,000xg for 5 min at 4°C and the supernatant was transferred into an Eppendorf tube. This step was repeated. The sample was then centrifuged at 20,000xg for 10 min at 4°C. The pellet was washed once in MOPS/IS. Mitochondria isolated from heart tissue was resuspended in 200µl and mitochondria isolated from brain tissue in 400µl MOPS-IS. Protein concentration was determined with by a Bradford protein assay (described in 3.3) and aliquots were frozen in liquid nitrogen and stored at -80°C.

Buffers:

MOPS-IS	225 mM Mannitol 75 mM sucrose 10 mM MOPS (pH 7.2) 1 mM EDTA (pH 8.0)
add fresh	1 mM PMSF Roche complete protease inhibitor
BSA/IS	MOPS-IS + 4 mg/ml BSA

3.3. Bradford protein assay

The Bradford protein assay was carried out to determine the protein concentration of isolated mitochondria.

A 48well plate was used and 48µl distilled water, 2µl of the sample to test and 800µl RotiQuant were pipetted into the wells. For the calculation of the protein concentration, a dilution series of 50µl Immunoglobulin G concentrations was incubated together with 800µl RotiQuant and was used as a reference. The analysis of the samples was performed with the help of Tecan Spark10M at the absorbance 595nm and calculated with the help of GraphPadPrism. Each sample was measured three times to calculate a more precise value.

3.4. Sodium dodecyl sulphate polyacrylamide gel electrophoresis (SDS-PAGE)

Sodium dodecyl sulphate polyacrylamide gel electrophoresis (SDS-PAGE) was used to separate proteins according to their specific mass. SDS-Gels with a 10% Acrylamide Separation and a 4.5% Acrylamide Stacking were prepared as followed. First, the separation gel was poured between two glass plates and was covered with isopropanol. After polymerisation of the separation gel, the isopropanol was removed, and the stacking gel was added.

For sample preparation, mitochondria were spun for 5 min at 21,130xg at 4°C. Afterwards per 1 microgram (µg) of protein 1µl of 1xLaemmli buffer with 1% β-Mercaptoethanol was added to the pallet. The sample was resuspended and incubated in a shaker for 10 min at 1000rpm at 50°. Samples were centrifuged for 5 min at 21,130xg at room temperature before storing at -20°C or direct use.

The SDS-Gels were loaded with 4µl of protein marker (PageRuler Plus prestain protein ladder, ThermoFischer) and 10µg protein per lane. The SDS-Page then ran at 120 millivolt (mV) for 1½ hours (h) in a biorad SDS-gel system with 1x MOPS-buffer or 1xMES-buffer, depending on the gel and proteins analysed. Afterwards the SDS-gel was semidry blotted on a PVDF membrane (described in 3.6).

Gel buffers:

Separation (10% Acrylamid)	5 ml 30% Acrylamid
	5 ml Bis Tris 1 M (pH 6.4)
	5 ml distilled water (dH_2O)
(to start polymerisation)	75 µl 10% APS
	7.5 µl TEMED
Stacking (4.5% Acrylamid)	1.5 ml 30% Acrylamid
	3.3 ml Bis Tris 1 M (pH 6.4)
	5.15 ml dH_2O
(to start polymerisation)	100 µl 10 % APS
	10 µl TEMED

Buffers:

10xMES-buffer	0.5 M MES
	0.5 M Tris
	1% SDS
	10.25 mM EDTA
10xMOPS-buffer	0.5 M MOPS
	0.5 M Tris
	1% SDS
	10.25 mM EDTA

Sample buffer:

1x Lämmli	60 mM Tris (pH 6.8)
	2% SDS
	10% Glycerol
	1% β-mercaptoethanol
	0.01% Bromphenolblue

3.5. Blue native polyacrylamide gel electrophoresis (BN-PAGE)

The blue native polyacrylamide gel electrophoresis (BN-PAGE) was used to analyse protein complexes. The BN-Gels had a concentration gradient of 4-13% acrylamide and digitonin was used as a detergent. 50 µg protein per lane was used and 50µl of the protein mixture no.17044501 from Amersham, GE healthcare was used as marker proteins. All buffers and the BN-Gel were cooled before use and all steps were performed at 4°C.

First, the mitochondria were spun at 21,130xg for 5 min and 4°C. The pellet was resuspended 20 times with 50µl Digitonin Buffer and incubated for 30 min on ice. Afterwards the sample was spun at 21,130xg and 4°C for 10 min. The supernatant was transferred to a precooled tube. 5 µl of the 10x loading dye was added to the sample and centrifuged again for 5 min at 21,130xg and 4°C. 50 µl of the sample was loaded per lane. The empty lanes were filled with Digitonin buffer and loading dye without proteins. The gel ran in 4 litres of 1x Anode buffer and 1x Cathode buffer with Coomassie G for about 15 min at 25 milliampere (mA)/Gel. Afterwards the Cathode buffer was changed to the 1xCathode buffer (without Coomassie) and ran again at 25mA/Gel for ~45 min till the sample moved through the whole gel. The BN-gel was incubated in 1xSDS running buffer for about 5 min, before it was semidry blotted on a PVDF membrane (described in 3.6).

Gel buffers:

3xGel buffer	200 mM ε-Amino n-caproic acid 150 mM Bis-Tris /HCl (pH 7.0)
Acrylamide	49.5% T, 3% C (96 g Acrylamide, 3 g Bis-Acryl /200ml)

Sample buffers:

Digitonin buffer	1% digitonin (solved in dH_2O), 20 mM Tris-Cl (pH 7.4) 0.1 mM EDTA (pH 8.0) 50 mM NaCl 10% glycerol 1 mM PMSF
10x Loading Dye	5 % Coomassie blue G 500 mM E-amino n-caproic acid 100 mM Bis Tris (pH 7.0)

Acrylamid Gel (4-13%):

%	4	13	Stack
3xGel buffer (ml)	3	3	2.5
Acrylamide (ml)	0.73	2.35	0.6
Glycerol (ml)	-	1.8	-
Water (ml)	5.228	1.817	4.367
10% APS (µl)	20	20	60
TEMED (µl)	2	2	6

Buffers:

10x Anode buffer	500mM Bis/Tris/HCl (pH 7.0)
10x Cathode buffer	500mM Tricine 150mM Bis-Tris (pH 7.0) (0.2% Coomassie G)

3.6. Semidry Western Blot

The gels from SDS-PAGE (see 3.4) or the BN-PAGE (see 3.5) were transferred on a PVDF membrane with the help of a semidry transfer system (Owl Separation Systems, Inc. Mod.: 7332 HEP-1 from ThermoScientific). First, the gels were equilibrated in Transfer buffer and the PVDF membrane used, was activated with Ethanol and subsequently together with filter paper incubated in Transfer buffer. The western blot ran for 2 hours with 350mA. The blotted PVDF membrane was stained with the Stain, destained with Destain and then dried.

The membrane was stained with Coomassie and subsequently destained with Methanol. The membrane was blocked with 5% milk (with TBS-T) for 1h. Primary antibodies (in TBS-T + 5% milk) incubated for 2h. The membrane was washed 3 times for 5 min using TBS-T. Then, the membrane was incubated in secondary antibodies (in TBST + 5% milk) for 1h at RT. The development of the PVDF membranes was performed with SuperSignal West Pico PLUS Stable Peroxide (Ref.:1863099) and Luminol/Enhancer Solution (Ref.:1863098) from ThermoScientific and analysed using the Amersham Imager 600 from GE-healthcare.

Buffers:

Transfer buffer	20 mM Tris 150 mM Glycin 0.02% SDS 10% Ethanol
Stain	0.1% (w/v) Coommassie R-250 40% Ethanol 10% acetic acid 50% dH_2O
Destain	40% Ethanol 10% acetic acid 50% dH_2O
10xTBS (pH7.5)	200mM Tris/HCL 1.25M NaCl
TBS-T	1xTBS 1 ml/l Tween20

3.7. Co-Immunoprecipitation (CO-IP)

The Co-Immunoprecipitation (CO-IP) was used to precipitate FLAG-tagged proteins of the mitochondrial samples prepared with mitochondrial isolation (see 3.2.1). To bind these tagged proteins, FLAG beads (Ref.: M8823, millipore) and 3x FLAG peptides were used. The FLAG peptide is a synthetic peptide added to the C-terminus, N-terminus or the N-terminus preceded by a methionine residue (Met-FLAG®), and in internal positions of proteins. The amino acid sequence of 3xFLAG peptide from Sigma Aldrich (Ref.: F4799), used in this experiment, is Met-Asp-Tyr-Lys-Asp-His-Asp-Gly-Asp-Tyr-Lys-Asp-His-Asp-Ile-Asp-Tyr-Lys-Asp-Asp-Asp-Asp-Lys.[e]

The whole experiment was performed at 4°C. First, 1 microgram (mg) mitochondria were centrifuged at 21,130xg 5 min at 4ºC. The pellet was resuspended in 1 ml 1xIP solubilisation buffer with 1% Digitonin and 2mM PMSF. The samples were then incubated on ice for 30 min and were then centrifuged at 21,130xg for 10 min at 4ºC to remove any non-soluble material. 100µl of the supernatant was transferred into a new tube and 100µl 2x Lämmli was added. The sample was incubated on a shaker at 1,000 rpm and 50°C for 10 min and stored at -20°C.

In a mobicol "F" column (#M105035F), 40µl of FLAG beads (20 µl packed beads) in 50% slurry were equilibrated with 500µl 0.3% Digitonin IP solubilisation buffer and centrifuged at 100xg for 2 min at

[e] https://www.sigmaaldrich.com/catalog/product/sigma/f4799?lang=de&region=DE, 16.11.2020

4ºC. The samples were transferred into the column and incubated with gentle rotation at 4°C for 2 hours. Each sample was washed 8x each with 500µl 1xIP wash buffer with 0.3% digitonin at 46xg and 4°C and 1min. Finally, the bound protein was eluted by addition of 100 µl FLAG peptide (100µg/ml) in IP wash buffer containing 0.3% Digitonin. The sample was incubated at 4°C for 5 mins while shaking at 1000 rpm and afterwards eluted at 100xg for 1min. A second elution was performed with 50µl of the elution buffer on a shaker at 1400 rpm to remove any residual protein. Samples were pooled and 50 µl of 4x Lämmli buffer was added. Samples were then incubated on a shaker at 1,000 rpm and 50°C for 10 min and stored at -20°C.

Buffers:

5x IP solubilisation buffer	100mM Tris (pH7.4) 250mM NaCl 50% Glycerol 0.5mM EDTA (pH 8.0)
5x IP wash buffer	100mM Tris (pH7.4) 300mM NaCl 50% Glycerol 2.5mM EDTA (pH 8.0)

3xFLAG peptide (Sigma Aldrich, ref.: F4799)	4mg => 400µl TBS (pH7.4) dissolve in for 10mg/ml stock. Aliquot (10µl) and store at -20°C.

3.8. Transformation of *MACH1-T1 E.coli* cells

For bacterial transformation, 100µl competent *MACH1-T1 E.coli* bacteria were incubated with 20ng of plasmid DNA for 30 min on ice. Afterwards they were heat shocked for 1 min at 42°C and then put on ice for another 10 min. 300µl LB-Medium was added and then the bacteria were incubated 30 min at 700rpm and 37°C. 150µl of transformed bacteria were streaked on a LB-Ampicillin-plate (LB-Amp-plate) and incubated overnight at 37°C. Single colonies were picked and transferred in 5ml LB-medium with 100µg/ml Ampicillin. Bacterial cultures were grown over night at 37°C and 700rmp.

Agar-Plate/Medium:

LB-Amp-plate	1% w/v Tryptone 0.5% w/v Yeast Extract 0.1% NaCl 0.15% Agar Autoclave 20 min 121°C Add 100 µg/ml Ampicillin once solution is fairly cool
LB-medium	1% w/v Tryptone 0.5% w/v Yeast Extract 0.1% NaCl Autoclave 20 min 121°C
Ampicillin	100µg/ml

3.9. Plasmid isolation from *MACH1-T1 E.coli* cells

The Mini-Prep Kit with all solutions used was the PeqGOLD Plasmid Mini-Prep KitI from VWR LifeScience. The Mini-Prep was used to extract plasmid DNA out of *MACH1-T1 E.coli* bacteria.
The whole experiment was performed at room temperature.
First, the overnight bacterial culture (described in 3.8) was centrifuged for 10 min at 5,000xg in a 15ml Falcon tube. 250µl Solution I was added to the pellet and resuspended by vortexing. Afterwards the Solution I and the bacteria together with 250µl of Solution II were added into a fresh 1.5ml tube and mixed gently by inversion (10 times) till a clear lysate was obtained. Then the lysate was incubated 2min at room temperature. 350µl of Solution III were added and the samples were mixed by inversion till turning flocculent white (10 times). Then the sample was centrifuged at 10,000xg for 10 min at 22°C. The supernatant was transferred to a PerfectBind DNA Column in a collection tube. The Column in the collection tube was centrifuged at 10,000xg for 1 min at 22°C. The flow-through was discarded and the collection tube was kept for the further steps. The Columns were washed two times at 10,000xg for 1 min with 500µl of PW Plasmid Buffer and afterwards with 750µl of DNA Wash Buffer completed with Ethanol. The Column was dried at 10,000xg for 2 min and then 100 µl of sterile deionized water was added directly on the PerfectBind DNA Column matrix and incubated for 2 min. In the end, the column was put in a fresh Eppendorf tube and centrifuged at 5,000xg for 1min to eluate the DNA. The concentration of the eluted DNA was determined with the Tecan Spark10M at 260nm. The DNA was stored at -20°C.

3.10. Synthesis of radioactive precursor protein

The precursor protein was prepared with 10µl active [^{35}S]-Methionine. 10µg DNA together with 100µl TNT quick coupled transcription/translation system SP6 (TNTSP6) from Promega and the active Methionine were incubated for 1½ h at 25°C. The reaction was stopped by adding 16µl Methionine (0.2 M in dH_2O) and 25µl sucrose (1.5 M in dH_2O). The lysate was stored at -80°C until use.

3.11. Protein import into mitochondria

First, 200µg of isolated mitochondria prepared especially for the protein import (described in 3.2.2) were centrifuged at 21,130xg for 5 min at 4°C. The pellet was resuspended in 400µl Import buffer and incubated in a Thermo Shaker at 500rpm and 37°C for 2 min. The import was started by adding 20µl lysate to the sample incubating at 500rpm and 37°C and stopped at the indicated time points by transferring 120µl of the sample in the fresh cold tubes. Afterwards, the mitochondria were pelleted at 21,130xg for 5min at 4°C and the pellet was washed twice with 100µl import buffer.
Samples were analysed by BN-PAGE and SDS-PAGE (described in 3.4 and 3.5). The samples were solubilised in 60µl Digitonin buffer and incubated for 30 min on ice. After a centrifugation step at 21,130xg for 10 min at 4°C, the supernatant was taken to prepare the SDS and BN samples.

For the SDS-PAGE 10µl import sample and 2µl of 5xLämmli were mixed and incubated on a shaker at 1000rpm and 95°C for 5 min. 5µl of the sample was loaded on a 10%SDS-Gel and the gel ran in MES buffer at 120V for 1 hour (as described in 3.4).

For the BN-PAGE 50µl of the import sample was mixed with 5µl of 10x Loading Dye and was centrifuged at 21,130xg for 5min at 4°C. 50µl of the sample was loaded on a 4-13% acrylamide gel (as described in 3.5). The gel was destained in Destain overnight and afterwards washed with distilled water. The gel was dried with a 230VAC Serva, Hoefer Scientific Geldryer at 75°C for 1½ h. The marker was labelled with radioactive dye. Signals were detected by autoradiography using a Typhoon 9410 from GE healthcare.

Buffers:

Import buffer	250mM Sucrose 5mM Mg-acetate 80mM K-acetate 10mM sodium succinate 20mM Hepes-KOH (pH 7.4)
Add fresh	0.2 M ATP 1M DTT
Digitonin buffer	1% digitonin (recrystallized in EtOH), 20 mM Tris-Cl (pH 7.4) 0.1 mM EDTA (pH 8.0) 50 mM NaCl 10% glycerol 1 mM PMSF

3.12. Immunofluorescence

HEK293T cells were grown in 6-well plate to about 40% confluency. Coverslips were transferred into a 6-well plate and 200 µl Poly-L-lysine (1:10 diluted in PBS) was added. After 20 min incubation at room temperature, the wells were washed three times with PBS. Then the HEK293T cells were seeded into the wells with medium.

At 40% confluency, the medium was removed and a Mitotracker dilution (1:20,000 in normal growth medium) was added and incubated for 20 minutes at 37°C and 5% CO_2. The wells were washed with PBS three times and 1 ml 4% Paraformaldehyde was added. Fixation was carried out for 20 minutes at RT. The cells were washed three times with PBS. Cells were permeabilized using PBS + 0.1% Triton X-100 for 10 min at RT and washed three times with PBS. Then, the coverslips were transferred on a drop of PBS + 2% BSA on a parafilm and incubated 40 minutes at RT in the dark. The coverslip was washed seven times in PBS and then transferred on the primary antibody dilution in PBS + 2% BSA. The antibody incubated for 1h at 22°C in the dark. This process was repeated with the secondary antibody dilution. Afterwards the coverslip was washed again seven times in PBS and three times in water. The coverslip was transferred on mounting medium on a glass slide and incubated overnight at RT in the dark.

The next day the sample was analysed on the Leica DMi8 microscope.

Reagents:

	origin
Poly-L lysine	Sigma P4707-50ML
Medium (normal growth)	DMEM +10% FBS +Uridine
PBS (Phosphate-Buffered Saline)	GIBCO 20012-019
PBS + 0.1% Triton X-100	Sigma T-8787
Bovine seum albumin (BSA)	Sigma A6003
Roti-Mount Fluocare + DAPI	Roth HP20.1
Mitotracker Red CMXRos	Invitrogen M7512

3.13. Table of Antibodies

Primary Antibodies:

antibody	origin	Host species	Concentration (5% milk in TBS)
α-ATP5B	#4826, Rehling Lab	Rabbit	1:2000
α-COX4-I	#1522, Rehling Lab	Rabbit	1:500
α-DNAJC11	ab183518, abcam	Rabbit	1:500
α-FLAG	F1804-200UG, sigma	Mouse	1:500
α-MIC10	5032KB, UdS	Rabbit	1:500
α-MIC19	HPA 042935, sigma	Rabbit	1:500
α-MIC25	HPA 051975, sigma	Rabbit	1:500
α-MIC26	HPA003187, sigma	Rabbit	1:500
α-MIC27	HPA 000612, sigma	Rabbit	1:500
α-MIC60	5041 kb, UdS	Rabbit	1:500
α-QIL1	5037K1, UdS	Rabbit	1:500
α-SAM50	119/04, Mike Ryan	Rabbit	1:500
α-SLC25A46	ab237760, abcam	Rabbit	1:500
α-TOM22	ab179826, abcam	Rabbit	1:500
α-T-OXPHOS	MS604-300, abcam	Mouse	1:500
α-VDAC	PC548-50UG, millipore	Rabbit	1:500

Secondary Antibodies:

antibody	origin	Host species	Concentration (5% milk in TBS-T)
α-mouse (whole molecule) HRP conjugated GAM-POX-Ab	A4416, Sigma-Aldrich	goat	1:5000
α-rabbit IgG HRP (GoatPolyclonal) in 50% glycerol	AP187P, Merck EMD Millipore Corp.	goat	1:5000
Goat anti-Mouse IgG (H+L) Highly Cross-Adsorbed Secondary Antibody, Alexa Fluor Plus 488	A32723, Invitrogen	goat	1:500
Goat anti-Rabbit IgG (H+L) Highly Cross-Adsorbed Secondary Antibody, Alexa Fluor Plus 555	A32732, Invitrogen	goat	1:500

4. Results

4.1. Expression of MIC60 isoforms in different mouse tissues

I first examined different mouse tissues, to see if splice variants of MIC60 are expressed in different tissue types.[17,65,77] RNA sequencing presents different isoforms of MIC60, existing because of alternative splicing of the canonical MIC60 form. There are four described isoforms in humans and five described isoforms in mice (see Figure 2).[f]

Shown in Figure 4, I used mitochondria of mouse tissues to compare the expression of mouse MIC60 (mMIC60) isoforms. mMIC60 and mouse ATP5A (mATP5A) are analysed by a SDS-PAGE and Western Blot (as described in 3.2.1, 3.4 and 3.6). The C57BL/6J mouse mitochondria of different tissues were isolated and kindly provided by C.Maack (Laboratory of C.Maack, Cardiology UdS Homburg) and A.von der Malsburg (Laboratory of M. van der Laan, UdS Homburg).

As proposed by previous publications[17,65,77], the experiment with mouse tissues revealed the expression of two different mMIC60 isoforms in mouse heart, skeletal muscle and brain tissue. Shown in Figure 4, mMIC60 in mouse heart and skeletal muscle mitochondria has a smaller molecular mass compared to the molecular mass of mMIC60 in brain mitochondria. While the isoform of mMIC60 in the brain apparently has a molecular mass of approximately 85 kDa, the mMIC60 isoform in heart and skeleton muscle has a mass of about 75 kDa (Figure 4). This suggests that mMIC60 isoform 1 (mMIC60.1), the canonical sequence of the protein, with about 84 kDa mass, is present in mouse brain. The detected molecular mass of mMIC60 in heart and skeletal muscle shows the presence of another mMIC60 isoform in these tissues. It seems to be the isoform 3 (mMIC60.3), with a mass of around 78 kDa in mice. The other known isoforms of MIC60 in mice, mMIC60 isoforms 2, 4 and 5 have an either too small or too large molecular mass to be the experimentally verified mMIC60 isoform in heart and skeleton muscle (see Figure 2).[g]

The protein levels of mATP5A, a protein of the ATP synthase, was used for comparison of protein levels. The expressed levels of mMIC60 are proportional to the levels of mATP5A protein in the different mouse tissues and therefore seem to be expressed to a similar extent.

In summary, these results show, that mitochondria in different tissues contain different isoforms of mMIC60. mMIC60.1 in brain tissue and mMIC60.3 in heart and skeletal muscle.

Since the expression of MIC60.1 and MIC60.3 seems to be tissue specific and little is known about possible differences between those two isoforms, I decided to examine whether the different MIC60 isoforms are related to an alteration of MICOS and its interacting proteins.

[f] https://www.uniprot.org/uniprot/Q16891, 16.11.2020; https://www.uniprot.org/uniprot/Q8CAQ8, 16.11.2020
[g] https://www.uniprot.org/uniprot/Q8CAQ8, 16.11.2020

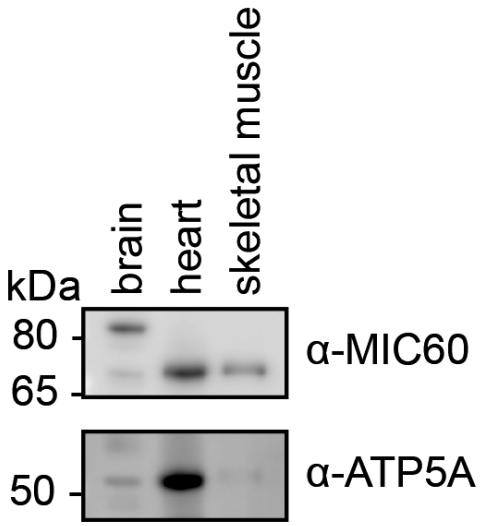

Figure 4
Comparison of MIC60 in mitochondria of different mouse tissues.
Proteins were analysed by an 8% acrylamide SDS-Gel using MOPS buffer to clearly separate the proteins by mass and then blotted with western blot. Antibodies against MIC60 and ATP5A were used.

4.2. Effect of FLAG-tagged MIC60 isoforms 1 and 3 on protein stability of other MICOS subunits

To analyse possible changes in mitochondria containing MIC60.1 and MIC60.3, cell lines expressing the different MIC60 isoforms were created. For this study, human embryonic kidney cells 293T (HEK293T cells) were used.

First, human MIC60 (MIC60) knockout cells were generated using the CRISPR/Cas9 system. The resulting deletion in the genome of these cells was located in the 5'UTR of the MIC60 mRNA, while the open reading frame itself remained intact. The MIC60 mRNA within these cells was therefore destabilised, resulting in a knockdown rather than a knockout. These cells were used to analyse the influence of MIC60 on MICOS, mitochondrial ultrastructure and function and to explore consequences of the expression of the MIC60 isoforms.

Described in publications before, the depletion of MIC60 leads to a destruction of the characteristic mitochondrial structure and a destabilisation of the MICOS complex as well as a downsizing of MICOS proteins.[31,34,37,38,54,70]

The MIC60 isoforms 1 and 3 were fused with a C-terminal FLAG-peptide (FLAG-tag) and expressed in the MIC60 knockdown cells (MIC60.1-F and MIC60.3-F). The rescued MIC60 proteins in the MIC60 depleted cells were used to identify changes in MIC60.1-F and MIC60.3-F expressing cells. To make sure that the expression of MIC60.1-F and MIC60.3-F in MIC60 depleted cells was successful, first an analysis of MIC60 and FLAG-peptide by SDS-Page and western blot was performed (described in 3.2.1, 3.4 and 3.6).

The cells with MIC60.1-F and MIC60.3-F express a lower protein amount of MIC60 than the wildtype cells, but nevertheless the isoform 1 and isoform 3 of MIC60 is detectable as well as the FLAG-peptide at the C-terminus of MIC60 (Figure 5a). As described before, there is a low amount of MIC60 protein detectable in the knockdown MIC60 cells (Figure 5a).

Figure 5a shows, that the molecular mass of MIC60 in the MIC60.1-F cells is almost similar to the molecular mass of MIC60 in the HEK WT cells. The MIC60.1-F plasmid was sequenced beforehand. Therefore, MIC60 isoform 1 is expressed in the WT and MIC60.1-F cells. MIC60.1-F has a molecular mass of about 85kDa. It migrates at a higher molecular weight than the canonical MIC60 isoform 1 (84kDa) due to the FLAG-peptide.

Also, the MIC60.3-F plasmid was sequenced beforehand, therefore it is known, that the MIC60.3-F cells express the MIC60 isoform 3. The MIC60.3-F cells express a MIC60 with a molecular mass of about 80kDa, so the molecular weight of MIC60 is smaller compared to the MIC60.1-F cells (Figure 5a).

The protein levels of TOM22, an outer membrane protein of the TOM complex, served as a loading control. Apparently, the expression of TOM22 is not influenced by the depletion of MIC60 and indicates, that there was a comparable amount of mitochondrial protein analysed. When comparing the detectable protein amount of MIC60 and FLAG-tag of the different cell lines, the detectable protein amount in HEK293T WT and MIC60.1-F cells is higher than in MIC60.3-F cells.

To analyse whether the two proteins localise to mitochondria, an immunofluorescence analysis was carried out (as described in 3.12). The cells were labelled with MitoTracker CMXRos (red), a fluorescent molecule, that accumulates in mitochondria in living cells. The FLAG-peptide present in the HEK293T cells expressing MIC60.1-F and MIC60.3-F was detected with a FLAG-antibody (green) and the nuclear DNA was labelled using DAPI (blue) (see Figure 5b).

In Figure 5b, the immunofluorescence in HEK293T WT cells shows a normal distribution of mitochondria and a weak, non-specific signal of FLAG-peptide. The MIC60.1-F and MIC60.3-F cells show a reduced but normally distributed amount of mitochondria and a specific FLAG-peptide signal. The merge (yellow), representing an overlap of mitochondria and FLAG-peptide, shows a proper targeting of the fusion protein inside the mitochondria of MIC60.1-F and MIC60.3-F cells (Figure 5b). There is no merge visible in the immunofluorescence of HEK293T WT cells. It seems like there is a colocalization of the expressed MIC60 isoforms with mitochondria. (Figure 5b).

All in all, the immunofluorescence shows the correct localisation of both MIC60 isoforms 1 and 3 inside the mitochondria.

5.a

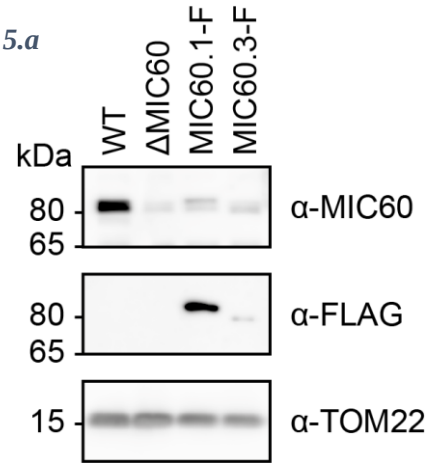

5.b

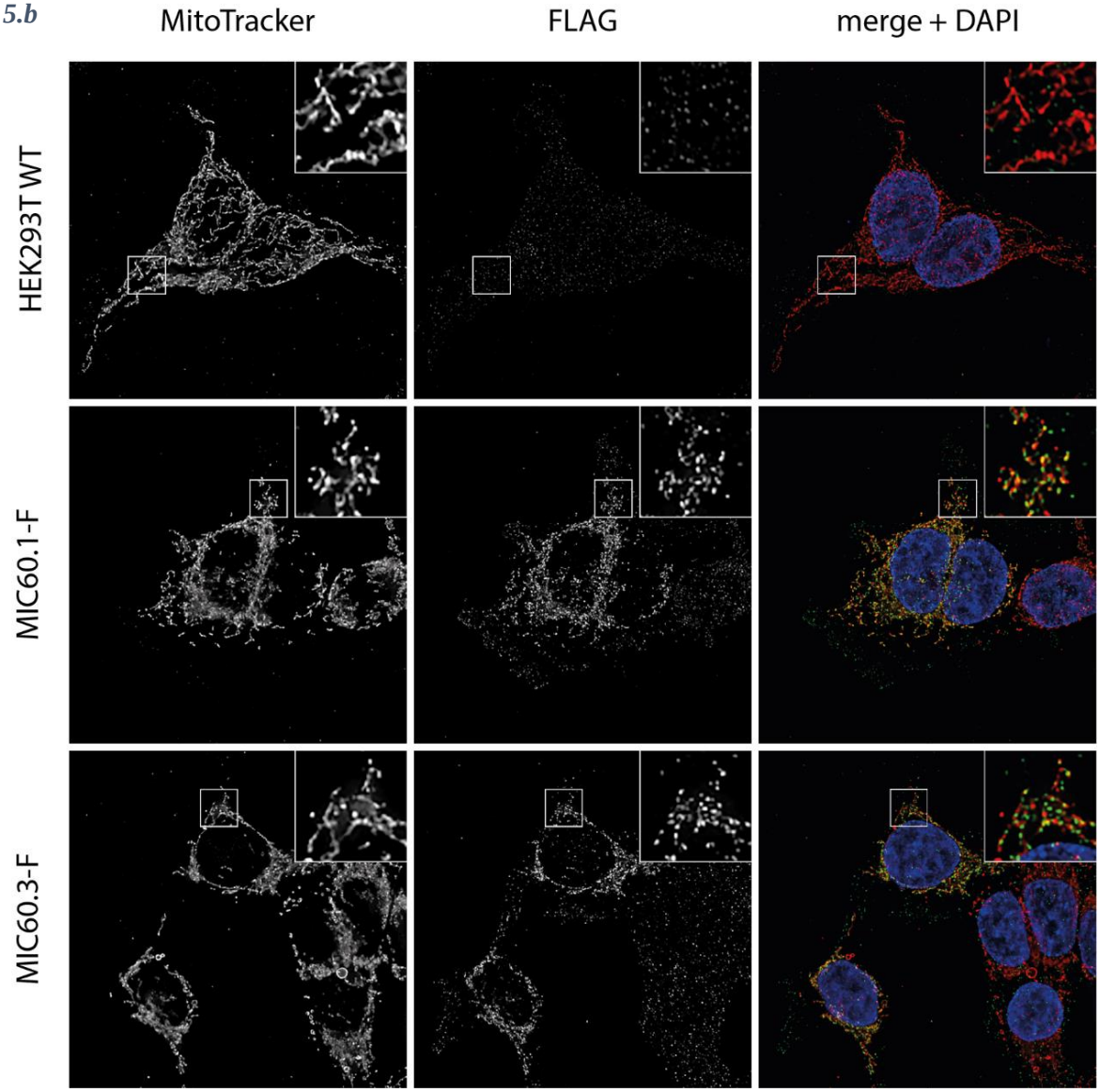

Figure 5

5.a - ***Analysis of protein stability in mitochondria of HEK293T cells with MIC60 knockdown and with expression of eighter MIC60.1 or MIC60.3 isoform tagged with FLAG-peptide.***
Proteins were analysed by an 8% acrylamide SDS-Gel run in MOPS buffer to separate the proteins by mass and then blotted with western blot. Antibodies against MIC60, FLAG-tag and TOM22 were used.

5.b - ***Immunofluorescence of HEK293T WT cells and of HEK293T cells expressing either MIC60.1-F or MIC60.3-F.***
MitoTracker (red), FLAG-peptide (green) and merge (yellow) +DAPI (blue).

To investigate possible changes in protein stability of MICOS subunits in the previously described cell lines with depleted MIC60 protein or different MIC60 isoforms, the mitochondria were isolated and prepared for SDS-Page and western blot analysis (described in 3.2.1, 3.3, 3.4 and 3.6)
First, to be able to address a change of the protein stability to the different cell lines, the knockdown of MIC60 was characterised. The knockdown of MIC60 has been described to result in a destabilisation of MICOS subunits as MIC60 is the core unit of MICOS complex.[31,38,48,70] An efficient knockdown of MIC60 is necessary to trace back the changes in the rescued MIC60 to the different isoforms.

As shown in Figure 6, MIC60 knockdown leads to the reduction of protein levels of all MICOS proteins – MIC10, QIL1, MIC12, MIC19, MIC25, MIC26 and MIC27. Furthermore, there is a lower amount of SAM50 present in those mitochondria lacking MIC60 (Figure 6). The outer membrane proteins DNAJC11, TOM22, SLC25A46 and VDAC are not affected by low MIC60 levels and there is no reduction of the respiratory chain proteins and the ATP-synthase proteins (Figure 6).

The difference in molecular mass between cells with MIC60.1-F and MIC60.3-F is visible (Figure 6). In both cell lines, the MIC60 isoforms are expressed in lower protein levels compared to the protein levels of MIC60 in WT cells. Especially the expression levels of MIC60 isoform 3 are very low. But the expression level of MICOS components largely reflects the expression level of MIC60.1-F and MIC60.3-F, therefore a comparison was still possible.
Comparing MIC60.1-F cells to WT cells, the protein stability of the MIB proteins seems to be similar (Figure 6). The loss of protein stability in MIC60 depleted cells is partially rescued (Figure 6). Furthermore, the protein stability of the outer membrane proteins, TOM22, SLC25A46 and VDAC and the inner membrane proteins of the respiratory chain complex and the ATP-synthase is comparable to the WT (Figure 6).
When comparing the MIC60.3-F cells to the WT cells, there seems to be no remarkable difference in the protein stability of the MIB complex (Figure 6). Like the MIC60 knockdown and the MIC60.1-F cells, there is no effect on outer membrane proteins, the respiratory chain complex proteins and the ATP-synthase proteins in MIC60.3-F cells (Figure 6). Therefore, the examined protein stability seems to be comparable in both rescued cell lines (MIC60.1-F and MIC60.3-F).

In conclusion, the depletion of MIC60 leads to lower protein levels of all MICOS complex proteins and the SAM complex. This underscores the role of MIC60 on the stability of MIB complex proteins which was shown previously in several studies.[31,38,48,70] Additionally, there is no direct impact of MIC60 on the outer membrane proteins and the oxidative parts of the mitochondria shown. The rescued cells with MIC60.1-F and MIC60.3-F both show a lower expression of MIC60 protein, nevertheless, the rescue was successful as both cell lines express a MIC60 isoform.

Furthermore, the protein stability of MICOS and MIB proteins is similar to WT cells. When comparing the different MIC60 isoforms, no difference regarding protein stability is detectable since protein levels are similar in the respective cell lines.

As the depletion of MIC60 is known to result in a destabilisation of the MICOS complex, analysing the complex stability, especially of MICOS and MIB, of the before described cells was a logical next step.

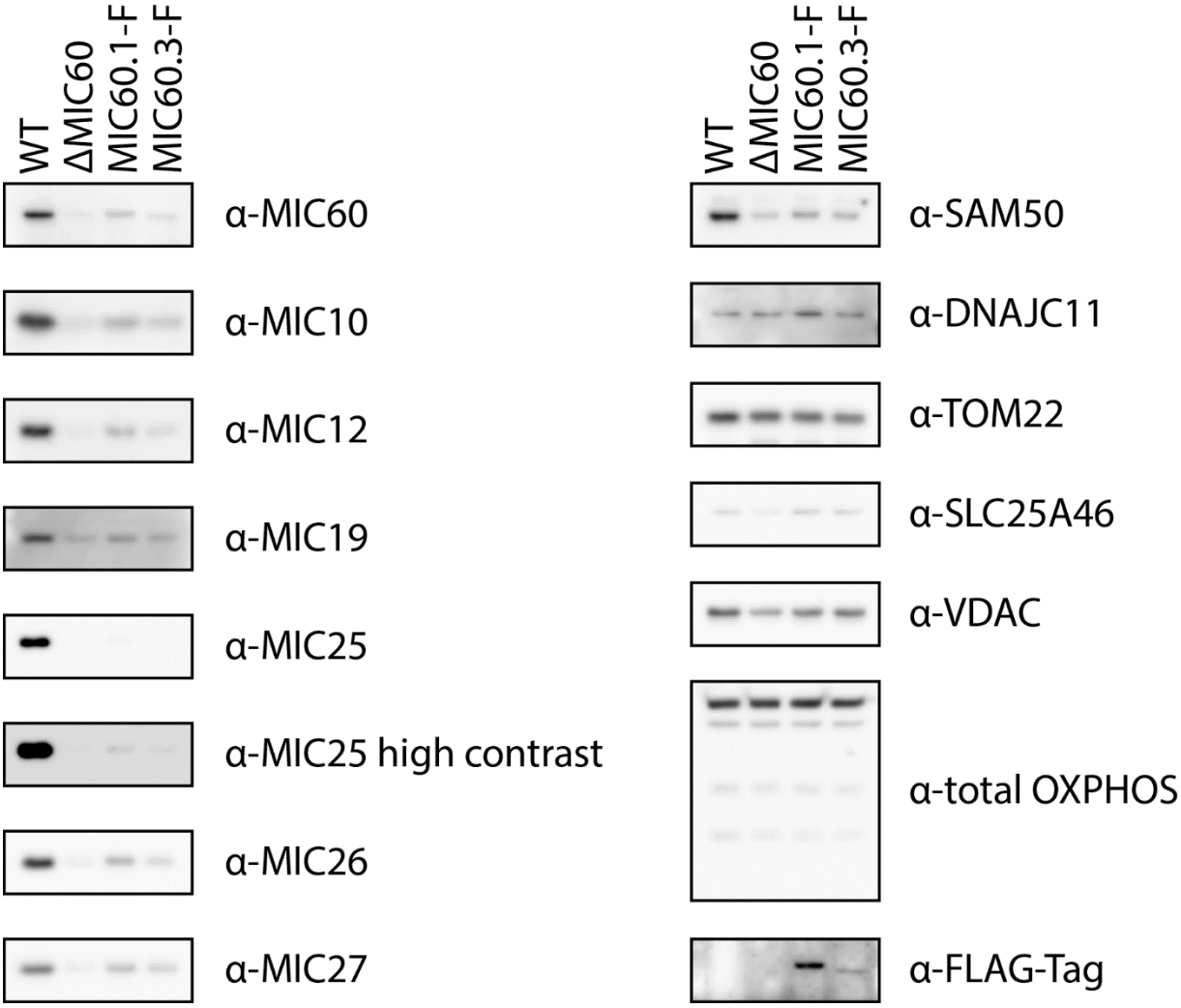

Figure 6

Analysis of protein stability in mitochondria of HEK293T with MIC60 knockdown and with expression of eighter MIC60.1 or MIC60.3 isoform tagged with FLAG-peptide.

Proteins were analysed by a 10% acrylamide SDS-Gel run in MES buffer to separate the proteins by mass and then blotted with western blot. Antibodies against MICOS complex proteins, MIB complex proteins and mitochondrial outer and inner membrane proteins were used.

4.3. Effect of FLAG-tagged MIC60 isoforms 1 and 3 on complex stability

The complex stability of previously described cells was analysed, focusing on the complex stability of MICOS and MIB complex, which are not known to be affected by the depletion of MIC60, as well as TOM complex and the ATP-synthase, a BN-PAGE was performed (described in 3.2.1, 3.5 and 3.6).

Figure 7 shows the destabilisation of the MICOS complex in cells lacking MIC60, as there is no complex detectable with antibodies directed against MIC60 (Anti-MIC60) and MIC10 (Anti-MIC10), the two core subunits of the MICOS complex. Likewise, the MIB complex is also affected by knockdown of MIC60. This is seen with the help of antibody against SAM-50 (Anti-SAM50) as part of the SAM and MIB complex. This underlines the findings in 4.2, showing a reduced protein stability of MICOS complex proteins and SAM50 in MIC60 knockdown cells. The depletion of MIC60 has no impact on the stability of the ATP-synthase in the inner mitochondrial membrane and does also not affect the TOM complex of the mitochondrial outer membrane (Figure 7).

When looking at the MIC60 rescue cells the MIC60.1-F cell line has a stable MICOS complex (Figure 7). The complexes of the MIC60.3-F cells are hardly detectable because of the low MIC60 protein expression levels of the MIC60.3-F cell line described in 4.2. Nevertheless, it looks like there is no change in complex stability compared to the examined complexes in MIC60.1-F cells. The FLAG-peptide is detectable in both cell lines which is included in a complex with a size of about 700kDa, most likely the MICOS complex (Figure 7). The cells with MIC60.1-F show the same complex stability as the HEK293T WT cells with a stable MICOS complex, confirmed by Anti-MIC60 and Anti-MIC10 and a stable MIB and SAM complex, confirmed by Anti-SAM50. The MICOS and MIB complexes in those cells are less abundant when compared to the WT cells (Figure 7).

In summary, the cells with MIC60 depletion show a destabilised MICOS complex. The rescue of MIC60 was successful as the results indicate a normal MICOS complex stability in the MIC60.1-F and MIC60.3-F cells. Comparing the two different isoforms of MIC60 and keeping in mind, that the expression level of MICOS components largely reflects the expression level of MIC60 isoforms, especially the low expression of MIC60.3-F, there is no difference in MICOS and MIB complex stability shown in this experiment.

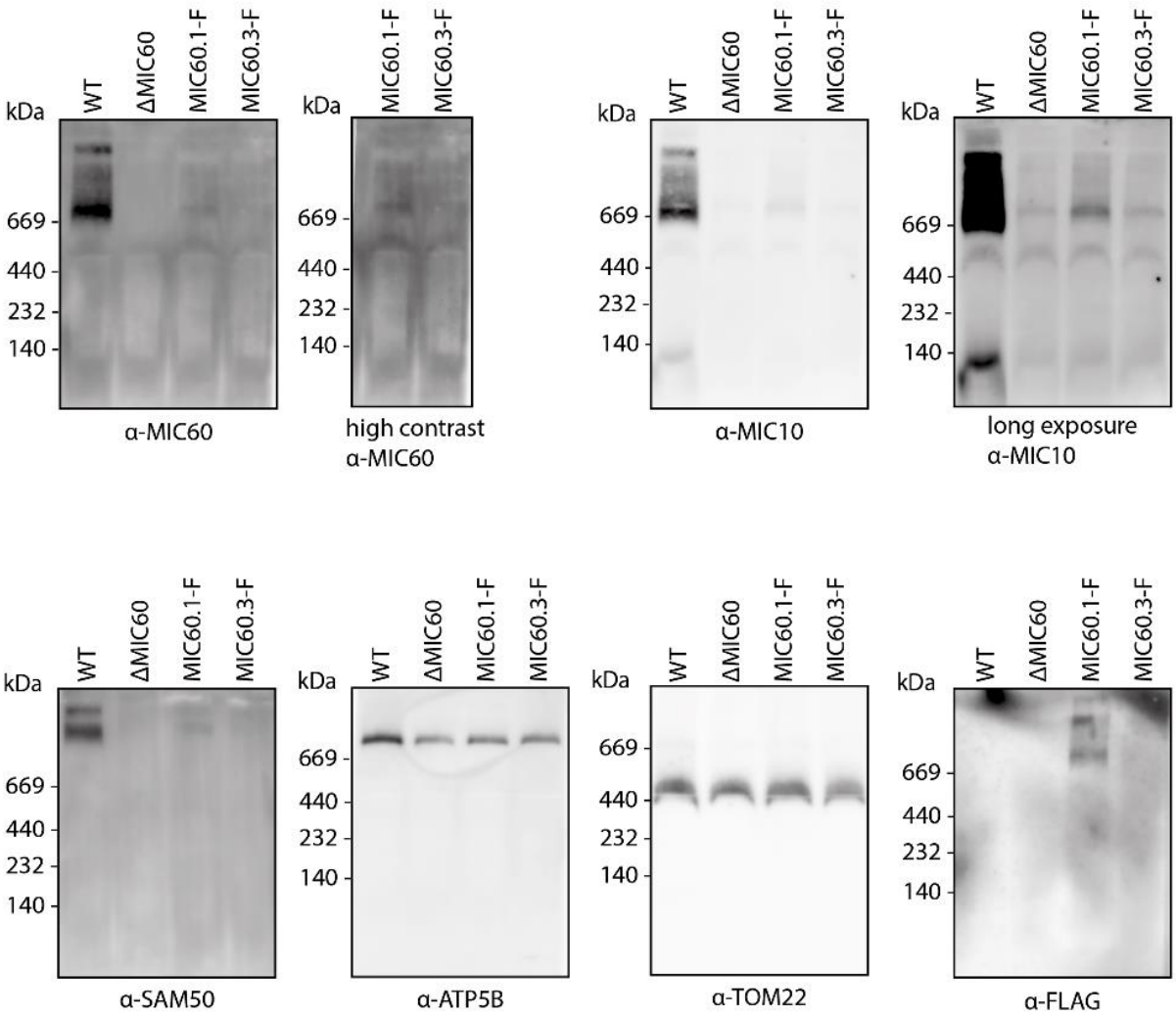

Figure 7

Analysis of complex stability in human mitochondria of HEK293T cells with MIC60 knockdown and with expression of eighter MIC60.1 or MIC60.3 isoform tagged with FLAG-peptide.

The complexes were analysed by a 4-13% BN-PAGE to separate the native complexes by mass and then blotted with western blot. Antibodies against MICOS complex, MIB complex, SAM complex and TOM complex and respiratory chain complex were used.

4.4. Effect of FLAG-tagged MIC60 isoforms 1 and 3 on protein-protein interactions

As the two different isoforms of MIC60 showed no change in protein stability and complex stability, protein-protein interactions were examined, since the different MIC60 isoforms might not interact with the same subset of proteins, which is not seen when detecting protein and complex stability.

To evaluate protein interactions of MIC60, the FLAG-tagged MIC60 was used for protein complex immunoprecipitation (CO-IP) (as described in 3.7), the FLAG-peptide was precipitated with anti-FLAG-beads from mitochondria lysates (described in 3.2.1). Afterwards the samples were analysed by SDS-PAGE and western blot (described in 3.4 and 3.6). The total represents a mitochondrial lysate while the eluate contained the precipitated proteins (described in 3.7).

The MIC60.1-F pull-down purifies the MICOS complex as well as the bound proteins and contains the MIB complex proteins SAM50 and DNAJC11 (Figure 8). The MIC60.3-F pull-down also purifies these proteins in a comparable amount, considering the lower amount of expressed MIC60.3-F in these cells. Neither SLC25A46 nor TOM22, two outer membrane proteins, are co-purified with MIC60.1-F and MIC60.3-F, indicating they might have a low affinity to the MICOS/MIB complexes containing MIC60.1-F and MIC60.3-F.

To summarise, there is no difference in protein-protein interaction when comparing MIC60.1-F and MIC60.3-F. The MIC60.3 seems to interact with the same proteins as the canonical MIC60.1.

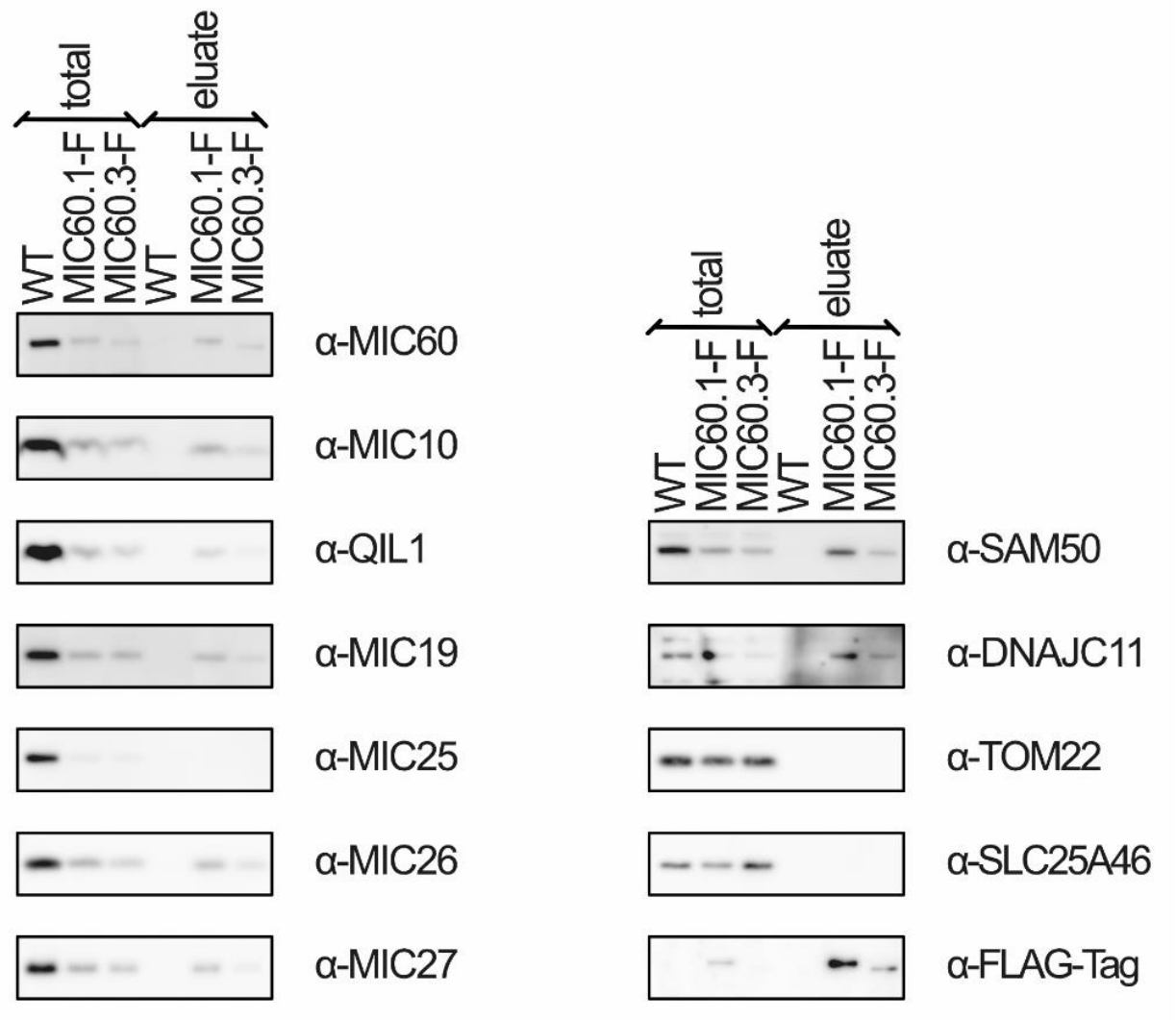

Figure 8

Analysis of protein-protein interactions in mitochondria of HEK293T cells with expression of eighter MIC60.1 or MIC60.3 isoform tagged with FLAG-peptide.

MIC60 protein-protein interactions were analysed by IP. Proteins were analysed by a 10% acrylamide SDS-Gel run in MES buffer to separate the proteins by mass and then blotted with western blot. Antibodies against MICOS complex proteins, MIB complex proteins and mitochondrial outer and inner membrane proteins were used.

4.5. Effect of MIC60 isoforms 1 and 3 on protein and complex stability

Since the C-terminal FLAG-peptide could influence protein and complex stability and the import of MIC60 into mitochondria, the FLAG-peptide could account for the low expression levels of MIC60.1-F and MIC60.3-F. Therefore, MIC60 knockdown cells in which MIC60 isoform 1 and 3 without a FLAG-peptide were reintroduced (MIC60.1 and MIC60.3) (described in 3.1), reflecting the endogenous state of these proteins, were created. Isolated mitochondria were used for a SDS-PAGE and a BN-PAGE with a subsequent western blot analysis (as described in 3.2.1, 3.4, 3.5, 3.6).

For the MIC60 knock-down HEK293T cells, the experiments showed similar results to the experiments described before (4.2 and 4.3). Analysis by SDS-PAGE shows that the depletion of MIC60 leads to a decrease of protein stability in all the MICOS complex proteins and SAM50 (Figure 9). DNAJC11 and the examined outer and inner membrane proteins are not affected by the depletion of MIC60 (Figure 9). The complex analysis with BN-PAGE (Figure 10) in MIC60 depleted cells shows a destabilisation of the MICOS and MIB complex. The complex stability of the TOM complex and the ATP-synthase remains unaltered in cells with MIC60 depletion (Figure 10).

The MIC60.1 and MIC60.3 cells (Figure 9) express a lower MIC60 protein amount than the WT cells, never the less, MIC60.1 and MIC60.3 cells express a comparable amount of MIC60 protein, therefore an interpretation of effects on the stability of MICOS proteins is still possible. Furthermore, the expression level of MICOS subunits reflect the expression level of MIC60.1 and MIC60.3 As shown before, the difference of molecular mass between isoform 1 and isoform 3 in MIC60 is clearly visible (Figure 9). The protein stability of the MICOS components is similar in cells expressing MIC60.3 in comparison to the cells expressing MIC60.1. Neither the proteins of the MICOS complex nor SAM50, that are affected by the depletion of MIC60, show major differences when the two isoforms of MIC60 are expressed.

This confirms the findings discussed before. The proteins affected by depletion of MIC60, the MICOS complex proteins and SAM50, are both effectively rescued in the MIC60.1 and MIC60.3 cells. Furthermore, the cells expressing MIC60 isoform 3 seem to have the same protein stability of MICOS complex proteins, SAM50, DNAJC11 and the analysed outer and inner membrane proteins compared to the cells expressing MIC60 isoform 1.

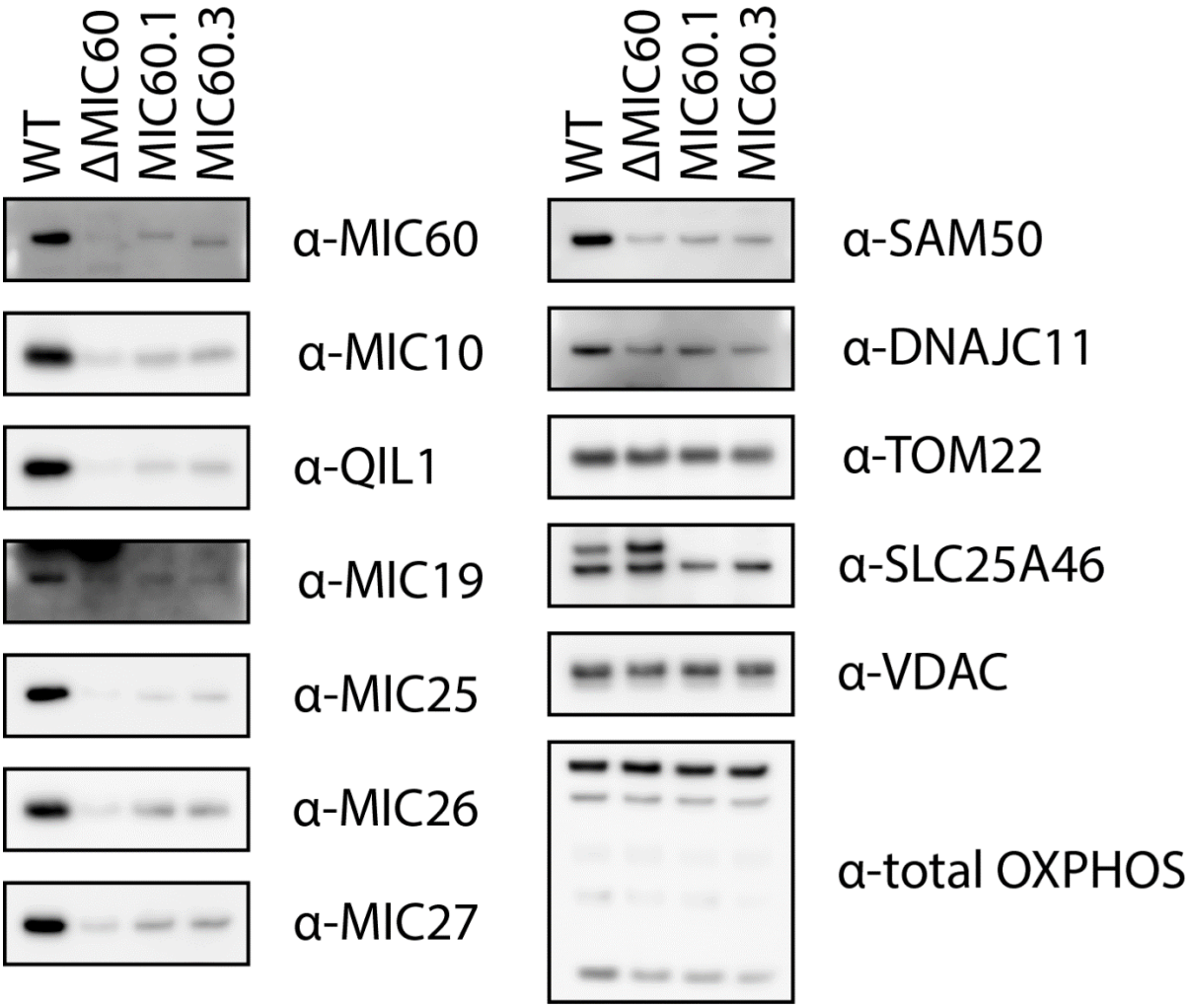

Figure 9
Analysis of protein stability in mitochondria of HEK293T cells with MIC60 knockdown and with expression of eighter MIC60.1 or MIC60.3 isoform.
Proteins were analysed by a 10% acrylamide SDS-Gel run in MES buffer to separate the proteins by mass and then blotted with western blot. Antibodies against MICOS complex proteins, MIB complex proteins and mitochondrial outer and inner membrane proteins were used.

The complex stability in these cell lines was analysed by BN-PAGE (Figure 10). Surprisingly, there seems to be a loss of complex stability or change in complex formation of MICOS complex in cells with MIC60.3. The MICOS complex of the cells expressing MIC60.3, shown with the help of Anti-MIC60 and Anti-MIC10, has a smaller molecular weight in comparison to the MICOS complex in WT and MIC60.1 mitochondria (see Figure 10, α-MIC60 and α-MIC10). The MIB complex is not affected as the molecular weight seems to be the same in MIC60.3 compared to MIC60.1 (Figure 10). Furthermore, the outer membrane complex TOM and the inner membrane F_1F_o-ATP-synthase are stable complexes in MIC60.3 cells, comparable to WT and MIC60.1 cells (Figure 10).

To sum it up, the HEK cells with MIC60.3 show a decrease of the molecular weight in MICOS complex. In HEK cells with MIC60.3-F, this smaller molecular weight of MICOS complex was not seen (described in 4.3).

Comparing the different MIC60 isoforms, there seems to be a difference in MICOS complex stability or composition in cells expressing isoform 3 in comparison to isoform 1.

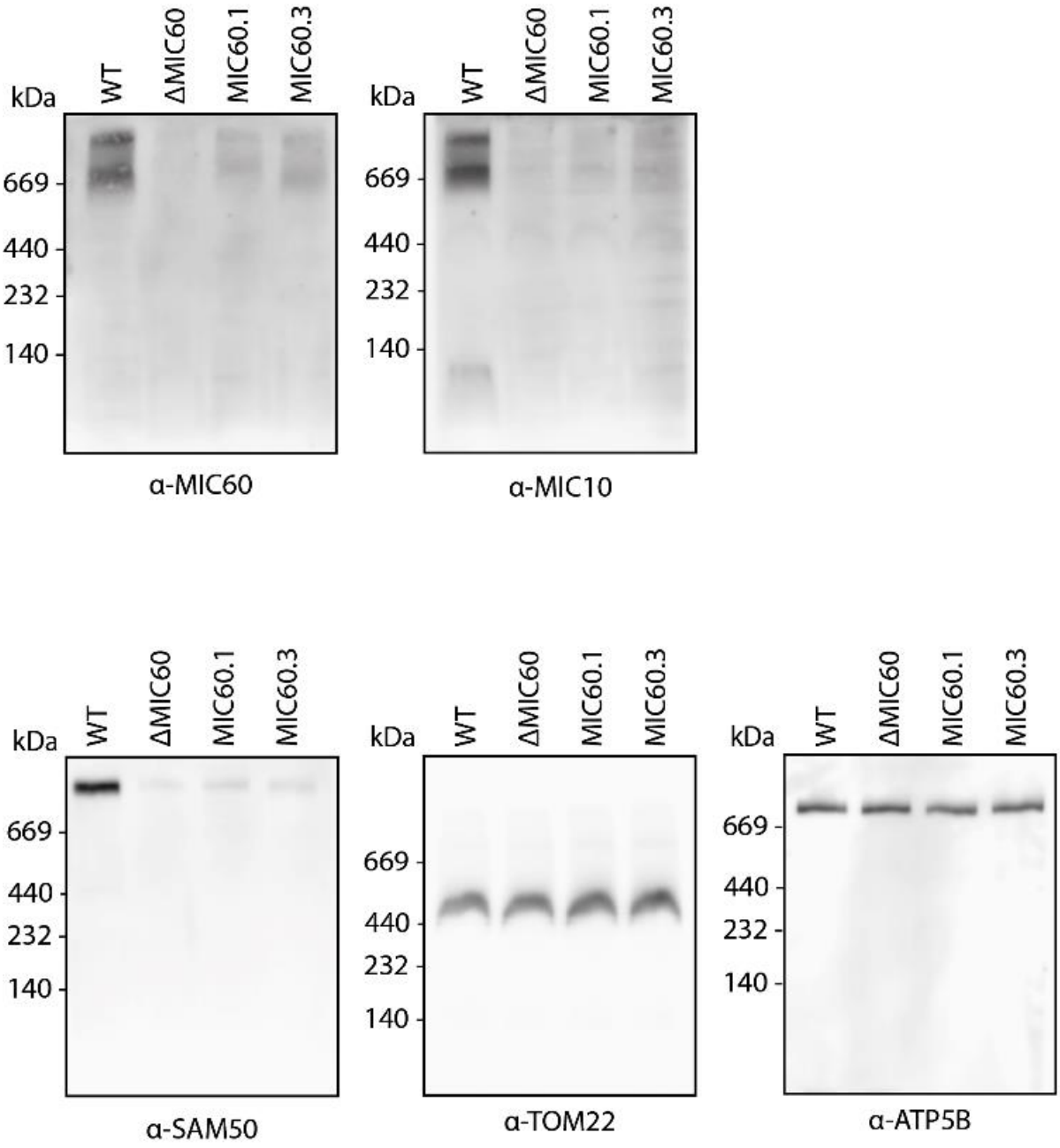

Figure 10

Analysis of complex stability in human mitochondria of HEK293T cells with Mic60 knockdown and with expression of eighter Mic60.1 or Mic60.3 isoform.

Complexes are analysed by a 4-13% BN-PAGE to separate the native complexes by mass and then blotted with western blot.

4.6. Effect of MIC60 isoforms 1 and 3 on protein import into mitochondria

The MICOS complex not only stabilises the inner membrane ultrastructure, but it also effects protein import through the outer mitochondrial membrane and assembly into the OM. MIC60 is largely involved as the interacting partner between MICOS, complex and SAM and TOM complex. In this experiment the β-barrel outer membrane complex VDAC, whose assembly into the outer mitochondrial membrane is performed by the TOM and SAM complexes, was used. To test whether the MIC60 depletion or different MIC60 isoforms have an effect on the function of SAM and TOM complex, the assembly of *in-vitro* translated, radioactively labelled VDAC-proteins in the outer mitochondrial membrane was tested in the HEK293T cell lines with depleted MIC60 and the rescued cells with MIC60.1 and MIC60.3 (described in 4.5).

As shown in Figure 11, the assembly of *in-vitro* translated VDAC, using [^{35}S]-VDAC, was analysed. Therefore, VDAC was *in-vitro* translated, in the presence of radioactively labelled Methionine and was than imported into purified mitochondria. The import was stopped at three different time points (5, 10 and 30 min) and the mitochondria were then analysed with the help of BN-PAGE to evaluate the complex assembly (described in 3.2.2, 3.5, 3.6, 3.8, 3.9, 3.10 and 3.11)

The time kinetic shows the assembly of VDAC in mitochondria isolated from HEK293T WT cells from an intermediate (I) complex to the mature (M) complex (Figure 11). This maturation is negatively affected in the MIC60 knockdown cells (Figure 11).

The MIC60.1 cells compared to the WT cells show the same efficiency of VDAC complex assembly and the same time kinetic, indicating that the MIC60 proteins in both cell lines function similarly (Figure 11).

Finally, the MIC60.3 cells form the same mature and intermediate complex with the same time kinetic as in WT cells and MIC60.1 cells (Figure 11). Therefore, the isoform 3 of MIC60 seems to function like MIC60.1.

These findings indicate that there is no difference in MIC60 isoforms 1 and 3 regarding their effect on β-barrel protein import into mitochondria.

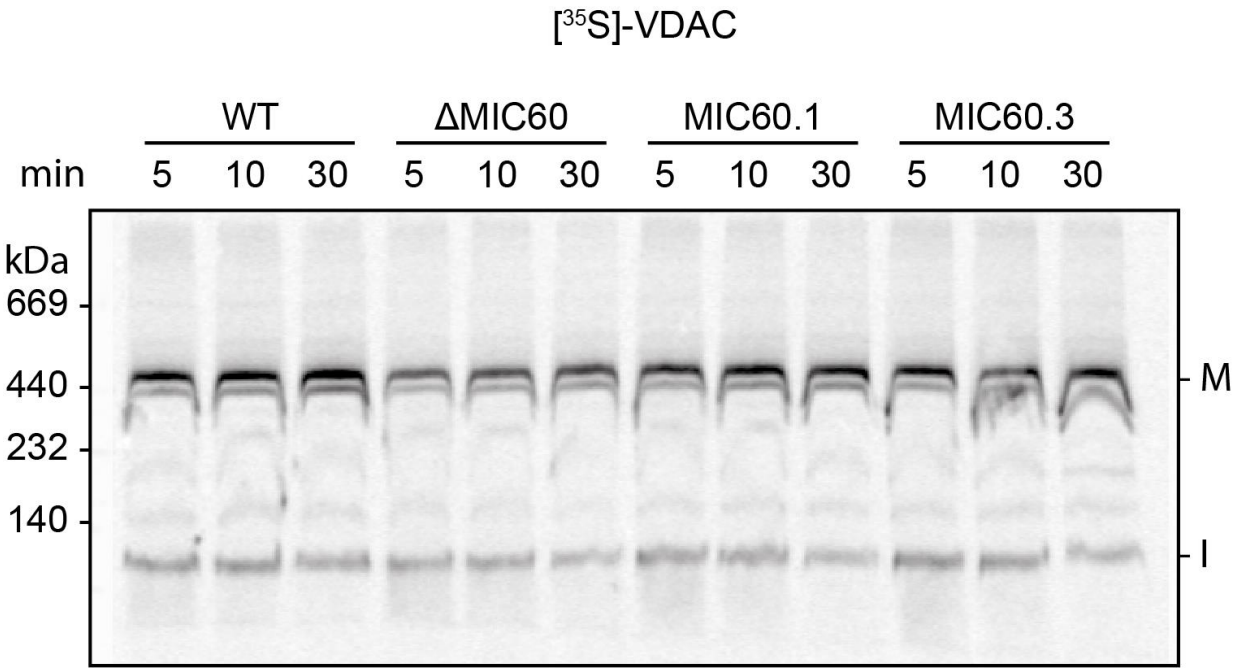

Figure 11
Analysis of VDAC import and assembly in human mitochondria of HEK293T cells with Mic60 knockdown and with expression of eighter Mic60.1 or Mic60.3 isoform.
S-methionine labelled VDAC was used to test VDAC complex assembly, assembly monitored after 5, 10 and 30 minutes VDAC complex forms mature complex (M) and intermediate (I).

4.7. Expression of MIC60 isoforms in RBM20 mutated mouse brain and heart tissues

For a detailed analysis of mMIC60 in different mouse tissues, I observed the protein stability and complex stability in mouse hearts and brains. The tissue samples were kindly provided by L.M. Steinmetz from the EMBL Heidelberg/Stanford Genome Technology Center. The Mitochondria were purified from frozen tissues by myself together with F.Wollweber (PZMS University Saarland AG M. van der Laan). Additionally to heart and brain tissue of a healthy WT mouse, tissue of a mouse with a heterogenic mutation of the RNA-binding motif protein 20 (RBM20) splicing factor was provided. RNA sequencing experiments in the group of L.M. Steinmetz revealed that mMIC60.3 was the predominant mRNA in the WT heart mitochondria and mMIC60.1 mRNA levels were increased in the heterogenic RMB20 mutated mice.
The isolated mitochondria were prepared separately for SDS-PAGE and BN-PAGE and were analysed by Semidry Western Blot (described in 3.2.3, 3.3, 3.4, 3.5, 3.6). As this was an analysis of mouse tissue, the following proteins will be labelled with a “m” for mouse.

The experiment shows a difference in the molecular mass of mMIC60 in the heart and brain mitochondria (Figure 12). The mMIC60 of brain cells has a higher molecular mass. These results are comparable to the first experiment (described in 4.1), leading to the conclusion of an expression of mMIC60.1 in brain and mMIC60.3 in heart cells. However, there is no difference seen in molecular

mass of the mMIC60 in WT mouse and RBM20 mutated brain and heart cells (Figure 12). Therefore, the mutation of RBM20 does not lead to robust expression of mMIC60.1 in mitochondria within heart cells.

Surprisingly, the analysis of the other mMICOS complex proteins, mSAM50 and the outer membrane proteins mDNAJC11, mSLAC25A46 and mVDAC as well as the respiratory chain complex and the mATP-synthase proteins, lead to some interesting findings.
First, the experiment shows a not detectable amount of mMIC19 in brain cells. Furthermore, an increase of mMIC25 protein level in brain cells is visible (Figure 12). In comparison, there is a lower amount of mMIC25 protein present in heart cells (Figure 12). When comparing the protein levels of mDNAJC11, there is more mDNAJC11 detectable in brain cells (Figure 12). Also, there are higher protein levels of the outer membrane protein mSLC25A46 visible in the brain cells (Figure 12). Here, the outer membrane protein mVDAC and the respiratory chain complex and the mATP-synthase proteins serve as a loading control, indicating that there is a comparable amount of mitochondrial proteins analysed (Figure 12).

At the protein level, the mMIC60 isoform in heart cells does not seem to be influenced by the heterogenic mutation of RBM20, as there is no change in mMIC60.3 to mMIC60.1 detectable. Nevertheless, the tissue specificity of mMIC60 isoforms is shown again. mMIC60.1 is expressed in brain cells and mMIC60.3 in heart cells. Higher expression levels of mMIC25, mDNAJC11 and mSLC25A46 can be found in brain cells, while there is an extremely low expression of mMIC19. Therefore, the protein expression of some MICOS complex and MICOS interacting proteins is changed depending on the tissue type.

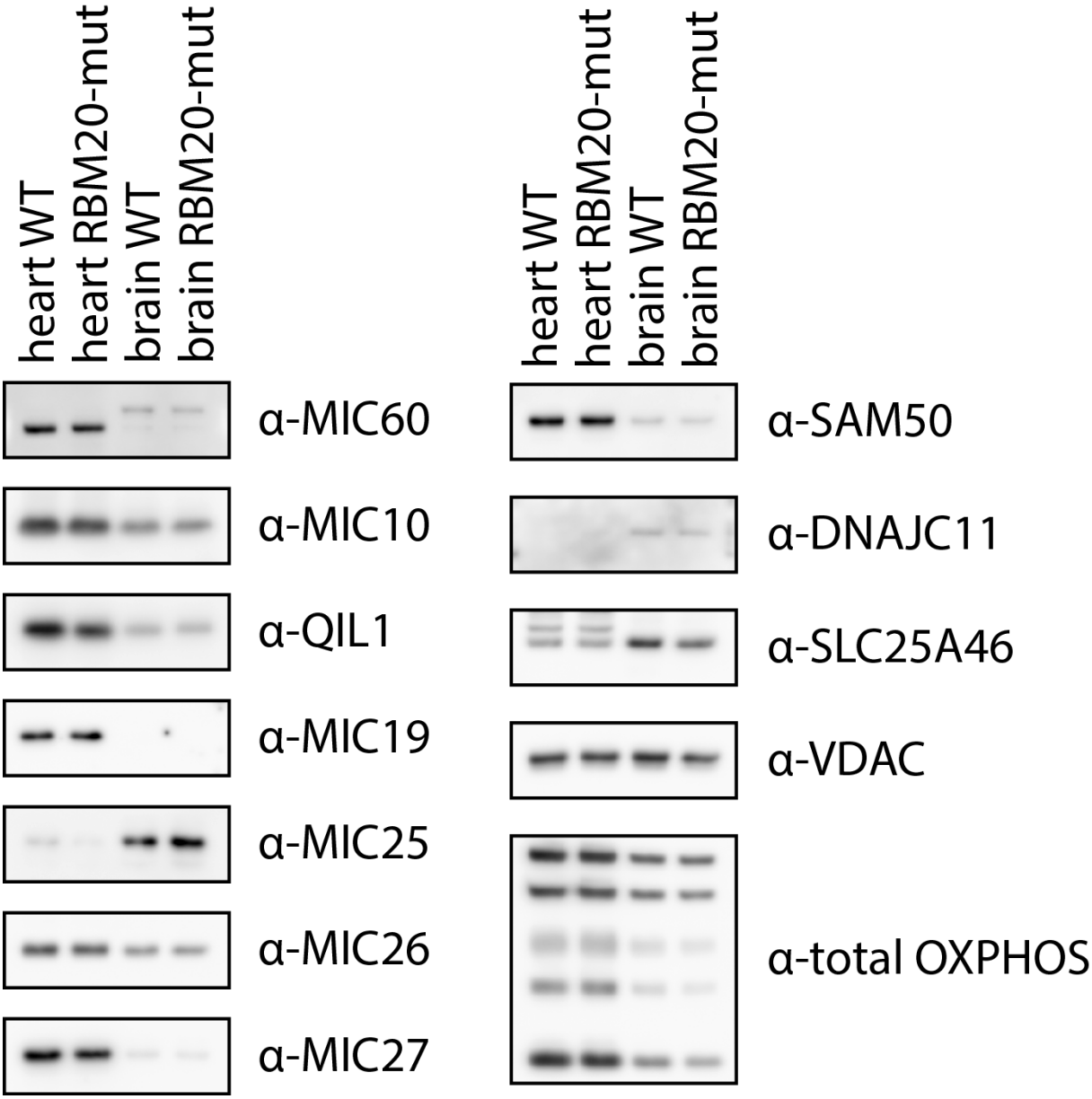

Figure 12

Analysis of protein stability in mitochondria of different mouse tissues and mouse breeds.

Proteins were analysed by a 10% acrylamide SDS-Gel run in MES buffer to separate the proteins by mass and were then analysed by western blot. Antibodies against MICOS complex proteins, MIB complex proteins and mitochondrial outer and inner membrane proteins were used.

When looking at the complex stability examined by BN-PAGE, both tissues seem to have stable complexes of MICOS and MIB as well as the inner membrane complex F_1F_o-ATP synthase and the cytochrome-C oxidase (COX), complex IV of the respiratory complex (Figure 13).

Strikingly, the MICOS complex in the heart tissue, detected by antibodies against MIC60 and MIC10, shows a decrease in molecular weight compared to the molecular weight of the MICOS complex in brain cells (Figure 13). Leading to similar results as shown in Figure 10. The molecular weight of the MICOS complex is smaller in cells with MIC60.3 compared to cells with MIC60.1. The molecular

weights of the MIB complex, F_1F_o-ATP synthase and Complex IV in mouse heart and brain cells are comparable to each other (Figure 13).

All in all, this experiment underlines the findings of earlier experiments in 4.5, showing a decrease of molecular weight of the MICOS complex MIC60.3 cells. Also, in mouse heart cells which expresses mMIC60.3, the molecular weight of the MICOS complex is decreased.

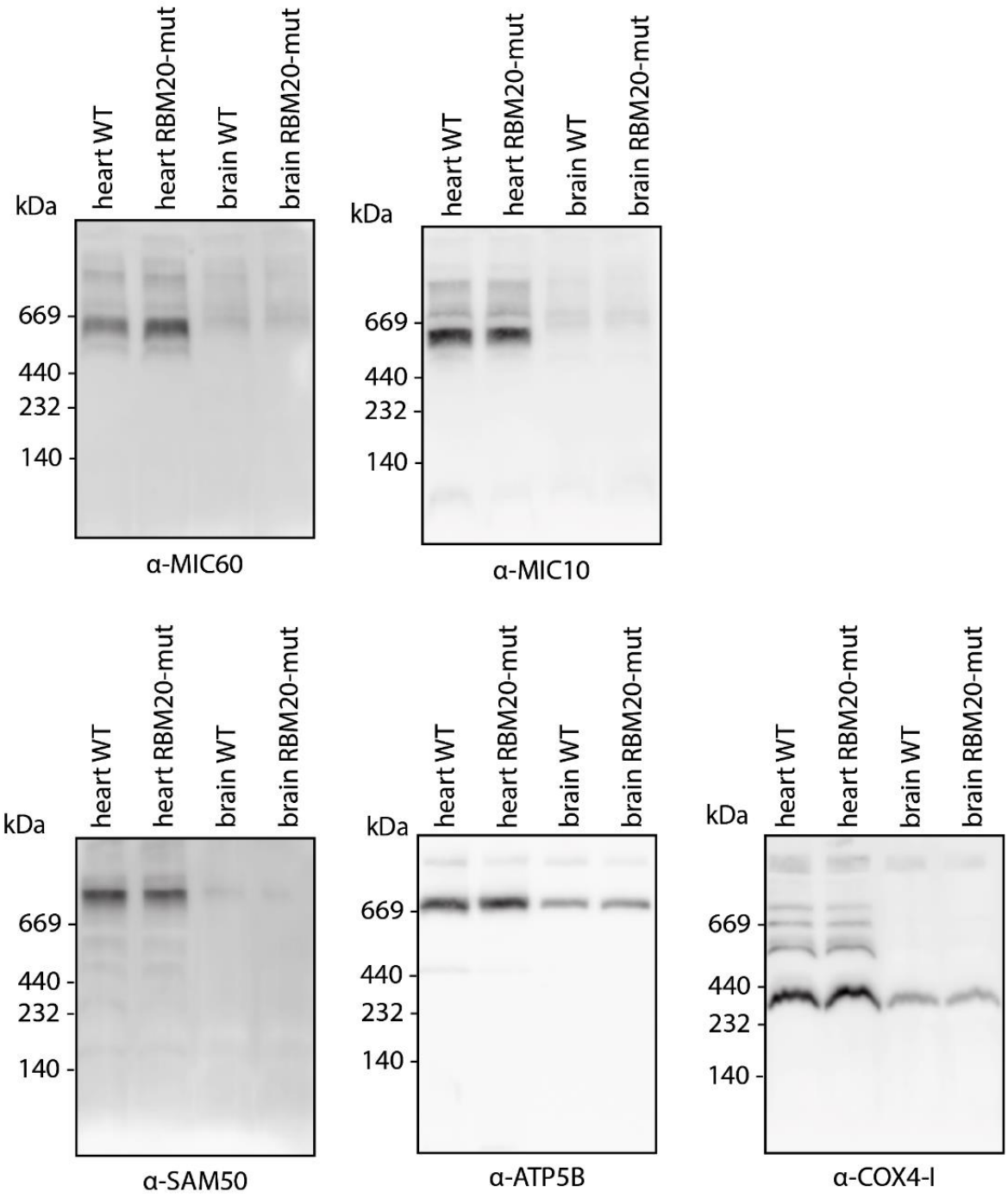

Figure 13
Analysis of complex stability in mitochondria of different mouse tissues and different mouse breeds.
Complexes are analysed by a 4-13% BN-PAGE to separate the native complexes by mass and then blotted with western blot.

5. Discussion

MICOS complex in mitochondria is necessary for the generation and stabilisation of cristae structures and the interaction of inner and outer mitochondrial membrane.[31,38,52] Therefore, stable MICOS protein levels and a stable MICOS complex is required for the maintenance of the characteristic structure of the mitochondria. MIC60 as a main component of MICOS plays a pivotal role in contributing to mitochondrial function in all kinds of tissues. MIC60 is proposed to appear in different isoforms depending on different tissue types.[17,65,77] So far it was not analysed whether the different isoforms of MIC60 differ in their mitochondrial function.

The analysis of MIC60 in different mouse tissues revealed a tissue specific expression of different mMIC60 isoforms. The new findings of this analysis showed the expression of mMIC60.3 in heart and skeleton muscle cells while mMIC60.1 is expressed in brain cells. Unpublished data of mRNA sequencing done by our research partner[h] has shown, that there are different isoforms of MIC60 expressed in human tissue. This leads to the assumption, that healthy human heart and skeleton muscle mitochondria also express MIC60 isoform 3.

As isoforms of other proteins function differently, the idea evolved, to analyse whether there is a difference in MIC60 function comparing MIC60.1 and MIC60.3. Those possible differences could include a difference in MICOS complex formation or a difference in interaction of MICOS with other proteins like SAM complex proteins or TOM complex proteins. To make an exact analysis of MIC60 isoforms possible, HEK293T cells with a depletion of MIC60 were created. Afterwards MIC60.1 and MIC60.3 with and without FLAG-peptide were expressed in those cells, to make sure the intended isoform of MIC60 is present.
When comparing MIC60.1 and MIC60.3 fused with a FLAG-tag, there was no difference between the two MIC60 isoforms in MICOS protein stability, complex stability and protein-protein interaction detectable. Also in MIC60.1 and MIC60.3 cells without FLAG-tag, the import function of the β-barrel protein VDAC, which is reduced when depleting MIC60, does not differ in MIC60 isoforms 1 and 3. Therefore, I do not expect a destabilisation of the mitochondrial ultrastructure or any changes in mitochondrial function based on missing cristae formation due to the expression of different MIC60 isoforms in different cell types.
The expression of MIC60.1 and MIC60.3 with the tagged FLAG-peptide was rather weak inside the rescued cells. Probably there was a lower import of MIC60.1-F and MIC60.3-F into the mitochondria caused by the FLAG-peptide at the C-terminus of the protein making the protein longer as usual. Because of this, differences in protein and complex stability between the two isoforms are possibly not

[h] Information kindly provided by our research partner L.M. Steinmetz from the EMBL Heidelberg/Stanford Genome Technology Center

revealed. New cell lines without FLAG-peptide were created to get a higher expression of MIC60.1 and MIC60.3. Furthermore, a possible influence of the C-terminal FLAG-tag on the protein and complex stability had to be excluded.

The cell lines expressing MIC60.1 and MIC60.3 without the FLAG-peptide, revealed a change in MICOS complex stability visible in MIC60.3 cells. The decrease of protein mass of MICOS complex can be explained in two ways. One explanation could be the reduced mass of MIC60.3 (80 kDa) in comparison to MIC60.1 (83.6 kDa) which could lead to a decrease of the molecular mass of MICOS complex. Because several copies of MIC60 form the MICOS complex, it is possible that the difference sums up leading to a smaller molecular weight of MICOS complex with MIC60.3. A second and more likely alternative is the explanation, that there is at least one protein not identified which plays a role in forming the MICOS complex and is influenced by MIC60, and therefore the different isoforms of MIC60 lead to different expressions of protein amounts. This assumption would as well be in accordance with the postulation of several studies that the human MICOS contains additional subunits. [31,34,54]

RNA sequencing of our research partner has shown that a mutation within the splicing factor RBM20 leads to alternative splicing of mRNA, expressing MIC60.1 instead of MIC60.3 in human heart tissue. This RBM20 mutation is connected to serious familiar dilatative cardio myopathy.[i] Surprisingly, mice with a heterogenic mutation of RBM20 express a mMIC60 with the same molecular weight as the mMIC60 in healthy WT mice. The expected change of mMIC60 isoforms because of the heterogenic RBM20 mutation does not manifest on the protein level. This leads to the assumption that there is still an expression of a normally functioning RBM20, correctly splicing the RNA in mouse heart leading to an expression of mMIC60.3.

Nevertheless, the mouse WT heart and brain mitochondria were still of interest, as the analysis of protein and complex stability in mouse tissue with two different mMIC60 isoforms was possible. As expected, the presence of mMIC60.3 in mouse heart mitochondria and mMIC60.1 in mouse brain mitochondria was confirmed as there was a difference in molecular weight of expressed mMIC60 detectable. Furthermore, the protein complex analysis showed a decrease in molecular weight of the MICOS complex in mouse heart mitochondria expressing mMIC60.3. These results reassure the new findings made in HEK293T cells. The same two theories, firstly of a change in molecular mass because of the decreased mass of MIC60.3 compared to MIC60.1 and secondly because of at least one not identified protein of the MICOS complex, apply. As the decrease in molecular mass of MICOS complex is shown in two different cell lines and species, this change is probably a MIC60.3 specific change in MICOS

[i] Information kindly provided by our research partner L.M. Steinmetz from the EMBL Heidelberg/Stanford Genome Technology Center

complex formation or stability. Therefore, the second theory indicating the presence of at least one, so far unknown protein of the MICOS complex, appears to be more likely.

There are more surprising observations as the mouse brain cells express higher levels of mMIC25 than the mouse heart cells. In comparison to that, the expressed protein amount of mMIC19, which is a paralog of mMIC25, is nearly undetectable in brain mitochondria. This finding suggests a predominant role of mMIC25 in comparison to mMIC19 within brain mitochondria. As far as protein function is concerned, one can speculate that mMIC25 replaces mMIC19, as the function of mMIC25 is yet not fully discovered. In conclusion, there is a tissue specific expression of mMIC25 in brain tissue. Future studies should include an analysis of MIC25 function in mouse but also human brain mitochondria as part of the MICOS complex but also its function as an independent protein.
The tissue specific expression of mMIC25 could lead to a difference of MICOS complex formation and stability between mouse brain and heart cells and could account for the decrease of molecular mass in mMIC60.3 cells MICOS complex.
Even if the HEK293T cells with MIC60.3 show the same decrease of molecular mass in MICOS complex compared to the HEK293T cells with MIC60.1, the HEK293T MIC60.1 cells do not show a change in protein stability of MIC19 and MIC25 compared to the MIC60.3 cells. Therefore, the difference in molecular mass of MICOS seems to be MIC60 isoform specific.

Furthermore, there are higher protein amounts of mDNAJC11 expressed in mouse brain mitochondria compared to mouse heart mitochondria. As the function of DNAJC11 is not clear, one can only speculate on the physiological consequences. To learn more about this tissue specific increased expression of DNAJC11 detailed analyses have to be performed. They should include CO-IP, MICOS and MIB protein and complex stability with cells lacking DNAJC11.
Also, higher protein amounts of mSLC25A46 are expressed in brain mitochondria. SLC25A46 is linked to numerous neurodegenerative diseases. Therefore, a tissue specific induced expression of SLC25A46 in brain tissue seems logical. Further analysis should include a detailed analysis of SLC25A46 function and localisation in the mitochondria, as this is yet not fully discovered. As mutations of SLC25A46 also lead to peripheral neuropathy, an analysis of tissue specific expression of SLC25A46 in peripheral neurons would be another point of interest.

In summary, MIC60 has an important role when it comes to cristae formation and stabilisation, as MICOS and MIB proteins are highly affected by the depletion of MIC60. Therefore, MIC60 is essential for complex formation.
Considering the performed experiments, a tissue specific expression of MIC60 isoforms 1 and 3 can be shown. As mitochondria in different tissue types fulfil slightly different functions, one can conclude, that the different MIC60 isoforms are involved in these changes. The experiments performed show no

detectable differences in protein stability, complex stability and changes in protein import function. There is only a decrease in molecular mass of MICOS complex in cells (human and mice) expressing MIC60.3. Possibly, this smaller molecular weight of the MICOS complex is a consequence of the smaller molecular weight of MIC60.3 itself. More likely, there is a different, so far undiscovered subunit of MICOS which is influenced by the expression of MIC60 isoforms.
While the analysis did not reveal a significant functional difference between the two MIC60 isoforms, a RBM20 mutation found in patients with familiar dilatative cardiomyopathy, is assumed to change the MIC60 isoform expressed in heart tissue. Therefore, one could conclude, that the expressed protein amount of MIC60.1 and MIC60.3 in HEK293T cells was too low to differentiate between the two isoforms or another conclusion could be that, the change of MIC60 isoforms is just a side effect of RBM20 mutation and leads to no essential changes in mitochondrial function and therefore does not play a role in familiar dilatative cardiomyopathy.

To determine the role of MIC60 isoforms in healthy heart and brains and in patients with familiar dilatative cardiomyopathy, new approaches should be made in future studies. As homogenic mutated mice are not viable, future studies should include more experiments with heterogenic RBM20 mutated mice to make sure, that RBM20 mutation leads to a change of MIC60 isoform 3 to MIC60 isoform 1 in heart cells. An even better solution would be an analysis of MIC60 and MICOS protein and complex stability with tissues of RMB20 mutated patients.
Furthermore, I propose, that the different MIC60 isoforms differ not only in molecular mass of the MICOS complex, but consequently also in mitochondrial cristae formation. For further studies new cell lines expressing higher levels of MIC60.1 and MIC60.3 and FLAG-tagged cell lines have to be created and analysed.

One major finding is the tissue specific expression of MIC60 isoforms, MICOS proteins as well as its interaction partners DNAJC11 and SLC25A46. So far, I only examined brain and heart tissue in detail, therefore other tissues, especially skeletal muscle tissue expressing a huge number of mitochondria needs to be examined as well. Tissue specificity of MICOS proteins in general is a huge topic, which could lead to new insights, not only on tissue specific functions of these proteins but also on diseases linked to MICOS protein malfunctions.

All in all, my thesis once again emphasises the importance of MIC60 for the cristae formation and stabilisation. It confirms the tissue specific expression of MIC60 isoforms 1 and 3 and a difference between the isoforms, as MIC60 isoform 3 leads to a change in MICOS complex formation or stability. Consequently, better understanding of the differences in function between these isoforms should be one of the future goals.

6. References

1. Abdul KM, Terada K, Yano M, et al. (2000) Functional analysis of human metaxin in mitochondrial protein import in cultured cells and its relationship with the Tom complex. *Biochem Biophys Res Commun* 276:1028-1034
2. Abe Y, Shodai T, Muto T, et al. (2000) Structural basis of presequence recognition by the mitochondrial protein import receptor Tom20. *Cell* 100:551-560
3. Abrams AJ, Fontanesi F, Tan NBL, et al. (2018) Insights into the genotype-phenotype correlation and molecular function of SLC25A46. *Hum Mutat* 39:1995-2007
4. Abrams AJ, Hufnagel RB, Rebelo A, et al. (2015) Mutations in SLC25A46, encoding a UGO1-like protein, cause an optic atrophy spectrum disorder. *Nat Genet* 47:926-932
5. Acín-Pérez R, Fernández-Silva P, Peleato ML, Pérez-Martos A, Enriquez JA (2008) Respiratory Active Mitochondrial Supercomplexes. *Mol Cell* 32:529-539
6. An J, Shi J, He Q, et al. (2012) CHCM1/CHCHD6, novel mitochondrial protein linked to regulation of mitofilin and mitochondrial cristae morphology. *J Biol Chem* 287:7411-7426
7. Anand R, Strecker V, Urbach J, Wittig I, Reichert AS (2016) Mic13 is essential for formation of crista junctions in mammalian cells. *PLoS One* 11:1-19
8. Beraldi R, Li X, Fernandez AM, et al. (2014) Rbm20-deficient cardiogenesis reveals early disruption of RNA processing and sarcomere remodeling establishing a developmental etiology for dilated cardiomyopathy. *Hum Mol Genet* 23:3779-3791
9. Bohnert M, Zerbes RM, Davies KM, et al. (2015) Central Role of Mic10 in the Mitochondrial Contact Site and Cristae Organizing System. *Cell Metab* 21:747-755
10. Brauch KM, Karst ML, Herron KJ, et al. (2009) Mutations in Ribonucleic Acid Binding Protein Gene Cause Familial Dilated Cardiomyopathy. *J Am Coll Cardiol* 54:930-941
11. Callegari S, Müller T, Schulz C, et al. (2019) A MICOS–TIM22 Association Promotes Carrier Import into Human Mitochondria. *J Mol Biol* 431:2835-2851
12. Cheng H, Zheng M, Peter AK, et al. (2011) Selective deletion of long but not short cypher isoforms leads to late-onset dilated cardiomyopathy. *Hum Mol Genet* 20:1751-1762
13. Christen P, Jaussi R, Benoit R (2016) Zellkompartimente und Proteinsortierung. In: *Biochemie Und Molekularbiologie*. Berlin, Heidelberg: Springer Verlag; 2016:283-295.
14. Darshi M, Mendiola VL, Mackey MR, et al. (2011) ChChd3, an inner mitochondrial membrane protein, is essential for maintaining Crista integrity and mitochondrial function. *J Biol Chem* 286:2918-2932
15. Ding C, Wu Z, Huang L, et al. (2015) Mitofilin and CHCHD6 physically interact with Sam50 to sustain cristae structure. *Sci Rep* 5:16064
16. Eydt K, Davies KM, Behrendt C, Wittig I, Reichert AS (2017) Cristae architecture is determined by an interplay of the MICOS complex and the F1Fo ATP synthase via Mic27 and

Mic10. *Microb Cell* 4:259-272

17. Feng Y, Madungwe NB, Bopassa JC (2019) Mitochondrial inner membrane protein, Mic60/mitofilin in mammalian organ protection. *J Cell Physiol* 234:3383-3393
18. Gressner AM, Arndt T (2019) *Lexikon Der Medizinischen Laboratoriumsdiagnostik*. Berlin, Heidelberg: Springer Verlag; 2019.
19. Guarani V, Jardel C, Chrétien D, et al. (2016) QIL1 mutation causes MICOS disassembly and early onset fatal mitochondrial encephalopathy with liver disease. *Elife* 5:1-18
20. Guarani V, McNeill EM, Paulo JA, et al. (2015) QIL1 is a novel mitochondrial protein required for MICOS complex stability and cristae morphology. *Elife* 4:1-23
21. Guo W, Schafer S, Greaser ML, et al. (2012) RBM20, a gene for hereditary cardiomyopathy, regulates titin splicing. *Nat Med* 18:766-773
22. Harner M, Körner C, Walther D, et al. (2011) The mitochondrial contact site complex, a determinant of mitochondrial architecture. *EMBO J* 30:4356-4370
23. Hoppins S, Collins SR, Cassidy-Stone A, et al. (2011) A mitochondrial-focused genetic interaction map reveals a scaffold-like complex required for inner membrane organization in mitochondria. *J Cell Biol* 195:323-340
24. Horvath SE, Rampelt H, Oeljeklaus S, Warscheid B, Van Der Laan M, Pfanner N (2015) Role of membrane contact sites in protein import into mitochondria. *Protein Sci* 24:277-297
25. Huynen MA, Mühlmeister M, Gotthardt K, Guerrero-Castillo S, Brandt U (2016) Evolution and structural organization of the mitochondrial contact site (MICOS) complex and the mitochondrial intermembrane space bridging (MIB) complex. *Biochim Biophys Acta - Mol Cell Res* 1863:91-101
26. Icho T, Ikeda T, Matsumoto Y, Hanaok F, Kaji K, Tsuchida N (1994) A novel human gene that is preferentially transcribed in heart muscle. *Gene* 144:301-306
27. Ioakeimidis F, Ott C, Kozjak-Pavlovic V, et al. (2014) A splicing mutation in the novel mitochondrial protein DNAJC11 causes motor neuron pathology associated with cristae disorganization, and lymphoid abnormalities in mice. *PLoS One* 9
28. Johnston AJ, Hoogenraad J, Dougan DA, et al. (2002) Insertion and assembly of human Tom7 into the preprotein translocase complex of the outer mitochondrial membrane. *J Biol Chem* 277:42197-42204
29. Kojima R, Kakimoto Y, Furuta S, et al. (2019) Maintenance of Cardiolipin and Crista Structure Requires Cooperative Functions of Mitochondrial Dynamics and Phospholipid Transport. *Cell Rep* 26:518-528.e6
30. Koob S, Barrera M, Anand R, Reichert AS (2015) The non-glycosylated isoform of MIC26 is a constituent of the mammalian MICOS complex and promotes formation of crista junctions. *Biochim Biophys Acta - Mol Cell Res* 1853:1551-1563
31. Kozjak-Pavlovic V (2017) The MICOS complex of human mitochondria. *Cell Tissue Res*

367:83-93

32. Kozjak-Pavlovic V, Ross K, Benlasfer N, Kimmig S, Karlas A, Rudel T (2007) Conserved roles of Sam50 and metaxins in VDAC biogenesis. *EMBO Rep* 8:576-582
33. Kuszak AJ, Jacobs D, Gurnev PA, et al. (2015) Evidence of distinct channel conformations and substrate binding affinities for the mitochondrial outer membrane protein translocase pore Tom40. *J Biol Chem* 290:26204-26217
34. van der Laan M, Horvath SE, Pfanner N (2016) Mitochondrial contact site and cristae organizing system. *Curr Opin Cell Biol* 41:33-42
35. Lamant M, Smih F, Harmancey R, et al. (2006) ApoO, a novel apolipoprotein, is an original glycoprotein up-regulated by diabetes in human heart. *J Biol Chem* 281:36289-36302
36. Li D, Morales A, Gonzalez-Quintana J, et al. (2010) Identification of novel mutations in RBM20 in patients with dilated cardiomyopathy. *Clin Transl Sci* 3:90-97
37. Li H, Ruan Y, Zhang K, et al. (2016) Mic60/Mitofilin determines MICOS assembly essential for mitochondrial dynamics and mtDNA nucleoid organization. *Cell Death Differ* 23:380-392
38. von der Malsburg K, Müller JM, Bohnert M, et al. (2011) Dual Role of Mitofilin in Mitochondrial Membrane Organization and Protein Biogenesis. *Dev Cell* 21:694-707
39. Martin W, Kowallik K V. (1905) Über Natur und Ursprung der Chromatophoren im Pflanzenreiche. *Biol Cent* 25:593–604
40. McBride HM, Neuspiel M, Wasiak S (2006) Mitochondria: More Than Just a Powerhouse. *Curr Biol* 16:R551-R560
41. Melin J, Schulz C, Wrobel L, et al. (2014) Presequence Recognition by the Tom40 Channel Contributes to Precursor Translocation into the Mitochondrial Matrix. *Mol Cell Biol* 34:3473-3485
42. Messina A, Reina S, Guarino F, De Pinto V (2012) VDAC isoforms in mammals. *Biochim Biophys Acta - Biomembr* 1818:1466-1476
43. Mootha VK, Bunkenborg J, Olsen J V., et al. (2003) Integrated Analysis of Protein Composition, Tissue Diversity, and Gene Regulation in Mouse Mitochondria. *Cell* 115:629-640
44. Müller-Esterl W, Brandt U, Anderka O, Kerscher S, Kieß S, Ridinger K (2018) Zellen – Organisation des Lebens. In: *Biochemie*. Berlin, Heidelberg: Springer Spektrum; 2018:37-58.
45. Muñoz-Gómez SA, Slamovits CH, Dacks JB, Baier KA, Spencer KD, Wideman JG (2015) Ancient homology of the mitochondrial contact site and cristae organizing system points to an endosymbiotic origin of mitochondrial cristae. *Curr Biol* 25:1489-1495
46. Neupert W, Herrmann JM (2007) Translocation of Proteins into Mitochondria. *Annu Rev Biochem* 76:723-749
47. Nunnari J, Suomalainen A (2012) Mitochondria: In Sickness and in Health. *Cell* 148:1145-1159

48. Ott C, Dorsch E, Fraunholz M, Straub S, Kozjak-Pavlovic V (2015) Detailed Analysis of the Human Mitochondrial Contact Site Complex Indicate a Hierarchy of Subunits. Cobine PA, ed. *PLoS One* 10:e0120213
49. Ott C, Straub S, Götz M, et al. (2012) Sam50 functions in mitochondrial intermembrane space bridging and biogenesis of respiratory complexes. *Mol Cell Biol* 32:1173-1188
50. Park YU, Jeong J, Lee H, et al. (2010) Disrupted-in-schizophrenia 1 (DISC1) plays essential roles in mitochondria in collaboration with Mitofilin. *Proc Natl Acad Sci U S A* 107:17785-17790
51. Pfanner N, van der Laan M, Amati P, et al. (2014) Uniform nomenclature for the mitochondrial contact site and cristae organizing system. *J Cell Biol* 204:1083-1086
52. Pfanner N, Warscheid B, Wiedemann N (2019) Mitochondrial proteins: from biogenesis to functional networks. *Nat Rev Mol Cell Biol* 20:267-284
53. Rampelt H, Wollweber F, Gerke C, et al. (2018) Assembly of the Mitochondrial Cristae Organizer Mic10 Is Regulated by Mic26–Mic27 Antagonism and Cardiolipin. *J Mol Biol* 430:1883-1890
54. Rampelt H, Zerbes RM, van der Laan M, Pfanner N (2017) Role of the mitochondrial contact site and cristae organizing system in membrane architecture and dynamics. *Biochim Biophys Acta - Mol Cell Res* 1864:737-746
55. Ran FA, Hsu PD, Wright J, Agarwala V, Scott DA, Zhang F (2013) Genome engineering using the CRISPR-Cas9 system. *Nat Protoc* 8:2281-2308
56. Schägger H (1995) [12] Native electrophoresis for isolation of mitochondrial oxidative phosphorylation protein complexes. In: *Methods in Enzymology*. Elsevier; 1995:190-202.
57. Schorr S, van der Laan M (2018) Integrative functions of the mitochondrial contact site and cristae organizing system. *Semin Cell Dev Biol* 76:191-200
58. Smith LM, Kelleher NL (2013) Proteoform: a single term describing protein complexity. *Nat Methods* 10:186-187
59. Sokol AM, Sztolsztener ME, Wasilewski M, Heinz E, Chacinska A (2014) Mitochondrial protein translocases for survival and wellbeing. *FEBS Lett* 588:2484-2495
60. Tang J, Zhang K, Dong J, et al. (2020) Sam50–Mic19–Mic60 axis determines mitochondrial cristae architecture by mediating mitochondrial outer and inner membrane contact. *Cell Death Differ* 27:146-160
61. Tang ZZ, Sharma S, Zheng S, Chawla G, Nikolic J, Black DL (2011) Regulation of the mutually exclusive exons 8a and 8 in the CaV1.2 calcium channel transcript by polypyrimidine tract-binding protein. *J Biol Chem* 286:10007-10016
62. Trenchevska O, Nelson R, Nedelkov D (2016) Mass Spectrometric Immunoassays in Characterization of Clinically Significant Proteoforms. *Proteomes* 4:13
63. Violitzi F, Perivolidi V-I, Thireou T, et al. (2019) Mapping Interactome Networks of

DNAJC11, a Novel Mitochondrial Protein Causing Neuromuscular Pathology in Mice. *J Proteome Res* 18:3896-3912

64. Wallin IE (1927) *Symbionticism and the Origin of Species*. Baltimore: The Williams and Wilkins Company; 1927.
65. Wang Q, Liu Y, Zou X, et al. (2008) The hippocampal proteomic analysis of senescence-accelerated mouse: Implications of Uchl3 and mitofilin in cognitive disorder and mitochondria dysfunction in SAMP8. *Neurochem Res* 33:1776-1782
66. Weber TA, Koob S, Heide H, et al. (2013) APOOL Is a Cardiolipin-Binding Constituent of the Mitofilin/MINOS Protein Complex Determining Cristae Morphology in Mammalian Mitochondria. Cobine PA, ed. *PLoS One* 8:e63683
67. Wideman JG, Muñoz-Gómez SA (2016) The evolution of ERMIONE in mitochondrial biogenesis and lipid homeostasis: An evolutionary view from comparative cell biology. *Biochim Biophys Acta - Mol Cell Biol Lipids* 1861:900-912
68. Wiedemann N, Kozjak V, Chacinska A, et al. (2003) Machinery for protein sorting and assembly in the mitochondrial outer membrane. *Nature* 424:565-571
69. van Wilpe S, Ryan MT, Hill K, et al. (2000) Erratum: Tom22 is a multifunctional organizer of the mitochondrial preprotein translocase. *Nature* 408:616-616
70. Wollweber F, von der Malsburg K, van der Laan M (2017) Mitochondrial contact site and cristae organizing system: A central player in membrane shaping and crosstalk. *Biochim Biophys Acta - Mol Cell Res* 1864:1481-1489
71. Wyles SP, Li X, Hrstka SC, et al. (2016) Modeling structural and functional deficiencies of RBM20 familial dilated cardiomyopathy using human induced pluripotent stem cells. *Hum Mol Genet* 25:254-265
72. Xie J, Marusich MF, Souda P, Whitelegge J, Capaldi RA (2007) The mitochondrial inner membrane protein Mitofilin exists as a complex with SAM50, metaxins 1 and 2, coiled-coil-helix coiled-coil-helix domain-containing protein 3 and 6 and DnaJC11. *FEBS Lett* 581:3545-3549
73. Yu BL, Wu CL, Zhao SP (2012) Plasma apolipoprotein O level increased in the patients with acute coronary syndrome. *J Lipid Res* 53:1952-1957
74. Zerbes RM, Bohnert M, Stroud DA, et al. (2012) Role of MINOS in mitochondrial membrane architecture: Cristae morphology and outer membrane interactions differentially depend on mitofilin domains. *J Mol Biol* 422:183-191
75. Zerbes RM, Höß P, Pfanner N, van der Laan M, Bohnert M (2016) Distinct Roles of Mic12 and Mic27 in the Mitochondrial Contact Site and Cristae Organizing System. *J Mol Biol* 428:1485-1492
76. Zerbes RM, Der Klei IJ Van, Veenhuis M, Pfanner N, Laan M Van Der, Bohnert M (2012) Mitofilin complexes: Conserved organizers of mitochondrial membrane architecture. *Biol*

Chem 393:1247-1261

77. Zhu L, Yu J, Shi Q, et al. (2011) Strain-and age-related alteration of proteins in the brain of SAMP8 and SAMR1 mice. *J Alzheimer's Dis* 23:641-654

78. Zimorski V, Ku C, Martin WF, Gould SB (2014) Endosymbiotic theory for organelle origins. *Curr Opin Microbiol* 22:38-48

7. Acknowledgement

In diesem Zuge möchte ich mich bei allen bedanken, die maßgeblich an der Fertigstellung meiner Dissertation beteiligt werden.

Prof. Dr. Martin van der Laan für die Aufnahme in seiner Arbeitsgruppe und die Möglichkeit diese Arbeit unter seiner Aufsicht anzufertigen. Für die Gesprächsbereitschaft, Betreuung und Unterstützung bei fach- und fachübergreifenden Fragen, möchte ich mich an dieser Stelle herzlich bedanken.

Des Weiteren gebührt mein Dank Dr. Karina von der Malsburg und Dr. Alexander von der Malsburg für die herausragende Betreuung und Unterstützung, ihre guten Ratschläge und fachlichen Anregungen. Vielen Dank auch an Florian Wollweber für das Lösen so mancher inhaltlicher, experimenteller und sonstiger Probleme.
Ein großes Dankeschön an die komplette AG van der Laan und auch an die AG Mick, für die Aufnahme in das Team. Besonderer Dank gilt Katja Noll für die Einarbeitung im Labor und das Lösen so manchen experimentellen Problems, durch Ihre jahrelange Erfahrung.

Danke auch an Jenny Vögele für Ihre fachliche Meinung und Durchsicht des Manuskripts.

Zu guter Letzt möchte ich mich bei meinen Eltern, meiner Schwester und meinem Partner für die Unterstützung bedanken.